UNIVERSITY OF WEST ATTICA
FACULTY OF ENGINEERING
DEPARTMENT OF CIVIL ENGINEERING

Diploma Thesis

ACTIVE MASS DAMPER APPLICATION IN STEEL STRUCTURES

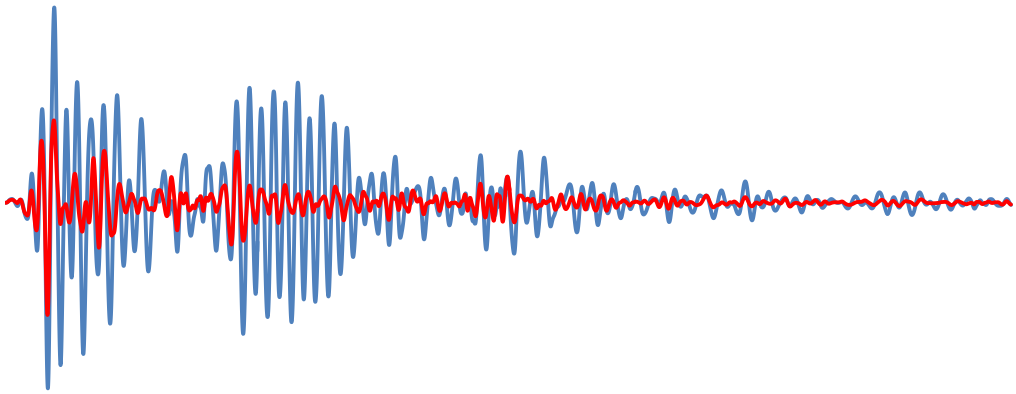

Student: Daktylidis I. Emmanouil-Ioannis
Registration Number: 445232017053

Supervisor

Nikolaos G. Pnevmatikos
Professor

ATHENS-EGALEO, FEBRUARY 2024

ΠΑΝΕΠΙΣΤΗΜΙΟ ΔΥΤΙΚΗΣ ΑΤΤΙΚΗΣ
ΣΧΟΛΗ ΜΗΧΑΝΙΚΩΝ
ΤΜΗΜΑ ΠΟΛΙΤΙΚΩΝ ΜΗΧΑΝΙΚΩΝ

Διπλωματική Εργασία

ΔΙΕΡΕΥΝΗΣΗ ΕΦΑΡΜΟΓΗΣ ΕΝΕΡΓΩΝ ΑΠΟΣΒΕΣΤΗΡΩΝ ΜΑΖΑΣ ΣΕ ΜΕΤΑΛΛΙΚΕΣ ΚΑΤΑΣΚΕΥΕΣ ΜΕ ΜΕΘΟΔΟΥΣ ΑΥΤΟΜΑΤΟΥ ΕΛΕΓΧΟΥ

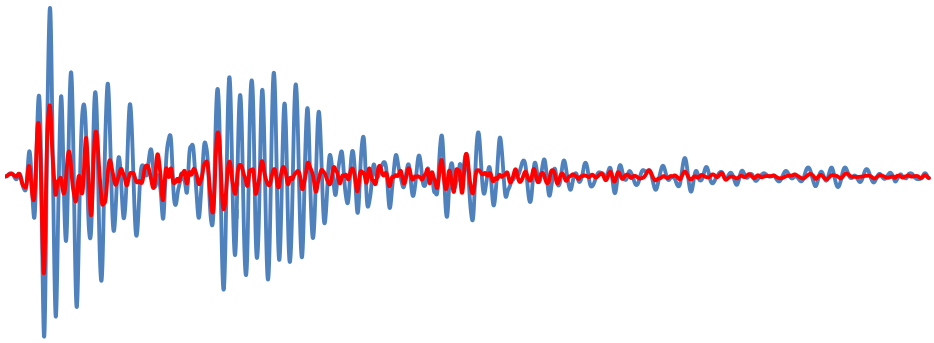

Φοιτητής: Δακτυλίδης Ι. Εμμανουήλ-Ιωάννης
ΑΜ: 445232017053

Επιβλέπων Καθηγητής

Νικόλαος Γ. Πνευματικός
Καθηγητής

ΑΘΗΝΑ-ΑΙΓΑΛΕΩ, ΦΕΒΡΟΥΑΡΙΟΣ 2024

Η Διπλωματική Εργασία έγινε αποδεκτή και βαθμολογήθηκε από την εξής τριμελή επιτροπή:

Νικόλαος Πνευματικός, Καθηγητής	Κωνσταντίνος Ρεπαπής, Αναπληρωτής Καθηγητής	Ισαάκ Βρυζίδης, Επίκουρος Καθηγητής
Nikolaos Pnevmatikos Digitally signed by Nikolaos Pnevmatikos Date: 2024.02.13 23:02:00 +02'00' (Υπογραφή)	Constantinos Repapis Digitally signed by Constantinos Repapis Date: 2024.02.13 23:42:55 +02'00' (Υπογραφή)	Isaak Vryzidis Digitally signed by Isaak Vryzidis Date: 2024.02.13 23:50:48 +02'00' (Υπογραφή)

ΔΗΛΩΣΗ ΣΥΓΓΡΑΦΕΑ ΔΙΠΛΩΜΑΤΙΚΗΣ ΕΡΓΑΣΙΑΣ

Ο κάτωθι υπογεγραμμένος Δακτυλίδης Εμμανουήλ Ιωάννης του Ιωάννη, με αριθμό μητρώου 445232017053 φοιτητής του Πανεπιστημίου Δυτικής Αττικής της Σχολής ΜΗΧΑΝΙΚΩΝ του Τμήματος ΠΟΛΙΤΙΚΩΝ ΜΗΧΑΝΙΚΩΝ,

δηλώνω υπεύθυνα ότι:

«Είμαι συγγραφέας αυτής της διπλωματικής εργασίας και ότι κάθε βοήθεια την οποία είχα για την προετοιμασία της είναι πλήρως αναγνωρισμένη και αναφέρεται στην εργασία. Επίσης, οι όποιες πηγές από τις οποίες έκανα χρήση δεδομένων, ιδεών ή λέξεων, είτε ακριβώς είτε παραφρασμένες, αναφέρονται στο σύνολό τους, με πλήρη αναφορά στους συγγραφείς, τον εκδοτικό οίκο ή το περιοδικό, συμπεριλαμβανομένων και των πηγών που ενδεχομένως χρησιμοποιήθηκαν από το διαδίκτυο. Επίσης, βεβαιώνω ότι αυτή η εργασία έχει συγγραφεί από μένα αποκλειστικά και αποτελεί προϊόν πνευματικής ιδιοκτησίας τόσο δικής μου, όσο και του Ιδρύματος.
Παράβαση της ανωτέρω ακαδημαϊκής μου ευθύνης αποτελεί ουσιώδη λόγο για την ανάκληση του διπλώματός μου.

Ο/Η Δηλών/ούσα

Δακτυλίδης Εμμανουήλ-Ιωάννης

Στην οικογένειά μου,

Ευχαριστίες

Με αυτή τη διπλωματική εργασία ολοκληρώνονται οι προπτυχιακές σπουδές μου στο Τμήμα Πολιτικών Μηχανικών της Σχολής Μηχανικών του Πανεπιστημίου Δυτικής Αττικής.

Με αφορμή αυτό, θα ήθελα να ευχαριστήσω πρωτίστως τον επιβλέποντα καθηγητή μου Δρ. Πνευματικό Νικόλαο για την υπέρ το δέον επιστημονική και ηθική υποστήριξη που μου παρείχε καθόλη την διάρκεια της εκπόνησης της διπλωματικής εργασίας και των σπουδών μου γενικότερα. Επίσης τον ευχαριστώ για όλες τις επιπλέον γνώσεις και εμπειρίες που μου παρείχε ανιδιοτελώς, αναφορικά με τον κόσμο της επιστήμης, της τεχνολογίας και της καινοτομίας. Στο πρόσωπό του γνώρισα τον ορισμό της επιτυχίας και της ευτυχίας βάσει κριτηρίων που δεν μετρώνται με κάποια από τις γνωστές μονάδες. Είναι μεγάλη τιμή για εμένα το ότι υπήρξα μαθητής του.

Τέλος, θα ήθελα να ευχαριστήσω την οικογένειά μου για την αμέριστη ηθική και υλική υποστήριξη καθ'όλη την διάρκεια των σπουδών μου, εκφράζοντας τον σεβασμό και την αγάπη μου προς αυτήν.

Περίληψη

Στην εργασία αυτή διερευνάται η επιρροή του ελέγχου στην απόκριση μεταλλικών κατασκευών που υπόκεινται σε σεισμική διέγερση. Η δυναμική φασματική ανάλυση είναι μία περίπτωση ανάλυσης κατασκευών που υπόκεινται σε σεισμό. Σε περιπτώσεις όμως που ο σεισμός υπερβαίνει το φάσμα σχεδιασμού η μόνη γραμμή άμυνας που διαθέτει η κατασκευή είναι η δυσκαμψία και η πλαστιμότητά της. Το αποτέλεσμα σε πολλές περιπτώσεις είναι σοβαρές υλικές ζημιές που καθιστούν το κόστος επαναλειτουργίας του κτηρίου μη βιώσιμο. Η λύση που προτείνεται σε αυτή την εργασία είναι η προσθήκη συσκευών αυτομάτου ελέγχου για την μείωση της απόκρισης της κατασκευής στα σημεία όπου αυτή υπερβαίνει το φάσμα σχεδιασμού. Η συσκευή ελέγχου που χρησιμοποιείται στην κατασκευή είναι ο ενεργός αποσβεστήρας μάζας (Active Mass Damper,AMD). Πραγματοποιούνται παραμετρικές αναλύσεις και διερευνάται η επιρροή της συσκευής ελέγχου τόσο σε συμμετρικές όσο και σε μη συμμετρικές μεταλλικές κατασκευές. Επιπλέον διερευνάται και η διαφορετική προσέγγιση της τοποθέτησης των συσκευών ελέγχου καθ' ύψος της κατασκευής σε διαφορετικούς προσανατολισμούς.

Λέξεις – κλειδιά

Ενεργός αποσβεστήρας μάζας, δυναμική φασματική ανάλυση, θεωρία ελέγχου, αντισεισμικός σχεδιασμός, μεταλλικές κατασκευές.

Abstract

This paper deals with the influence of structural control on steel structures subjected to earthquake excitation. Response spectrum analysis is one case of earthquake analysis in structures. In some cases, the earthquake applied exceeds the design spectrum. This way, the only defence against the excitation is the structure's ductility. In many cases, the result is severe damages that make the cost of rehabilitation unaffordable. The solution suggested in this paper is the design of a structure equipped with control devices. The control device applied to the models is the active mass damper (AMD). Parametric analyses are conducted in both symmetrical and non-symmetrical structures. Moreover, the simulation is extended to different approaches regarding the placement of the device in different floor levels and orientations.

Keywords

Active mass damper, response spectrum, design spectrum, structural control, earthquake engineering.

Table of Contents

List of tables

List of figures

1 Introduction

1.1 Seismic Structural Design in Greece

With the term ‘’design philosophy’’ someone can describe the fundamental principles of design. These principles are no more than selecting design loads and forces, analytical techniques and design procedures, preferences for specific structural system configurations and materials, and, last but not least, economic optimisation. The implementation of seismic design into buildings was first adopted in the 1920s and 1930s when the importance of inertial loads in buildings began to be recognised. However, in terms of data, the measurements of ground accelerations were neither reliable nor much at the time. On the other hand, little knowledge existed regarding the dynamic behaviour of structures to earthquake excitations. As a result, engineers applied 10% of the building’s weight as horizontal forces to the structure.

The first accelerograms became available in the 60’s. A more detailed examination of the seismic response of structures with multiple degrees of freedom was facilitated using new methods, such as the total resistance method and complex analytical procedures with computers. So, the previous seismic design based on the horizontal forces proved to be insufficient. Observations of buildings after actual earthquakes proved that the lack of strength did not always result in failure but could lead to significant damage. As a result, the structures could survive an earthquake with damages that, in most cases, owners could be economically repaired by the owners.

Following these observations that surplus strength is not essential and not necessarily desirable, the focus shifted from resisting large forces to "avoiding these forces", and the seismic design was now based on the ductile behaviour of the structure. Now, the main problem was the classification of the ductile deformations that lead to failure (shear ductile deformations) and those that provided ductility, which can be considered an essential characteristic when the structure undergoes seismic-induced deformations.

The Greek seismic code of 1959 introduced the design based on a seismic force acting at the centre of mass of each floor. This force resulted from the multiplication between vertical loads and a seismic coefficient, **ε**. The value depended on the seismic zone and the soil category of a construction area. The coefficient **ε** takes values between 0.04 and 0.16 depending on seismicity and soil hazard.

The way that seismic loads are distributed to the substructures is defined by the theory of monolithic elastic formation with rotation, assuming that the structure has diaphragmatic behaviour (each slab does not deform in its plane). The flexural stiffness and the geometry of the substructures define the centre of elastic rotation. From each substructure's flexural stiffness, the system's total flexural stiffness is also calculated for displacement x, y, and rotation ω around the centre of elastic rotation. Thus, the total displacement in each slab can be calculated based on the total flexure stiffness and the seismic load. The maximum displacements and flexural stiffness determine the shear forces in substructures. Then, the structural sufficiency of the structure can be checked based on allowable stresses.

The subsequent modifications in the seismic code were made in 1984. The introduction of the critical factors increased the seismic coefficient ε. The seismic load was now triangularly distributed by height to the building with the maximum value at the top. The seismic shear of the floor was distributed to the floors according to their flexural stiffness (monolithic theory). A significant modification of that era refers to the increase in seismic force for structural elements that lack lateral cover by infill walls. The most typical example is of the buildings with pilotis. In these cases, what was introduced is that if there is a reduction in infill walls on a floor by more than 25%, then an increase in the seismic force of each vertical element of that floor is made, equal to the percentage reduction of infill walls, and dense connectors are placed on the substructures throughout the height of the floor.

The latest major shift in the seismic design philosophy came in 1995 with the New Greek Seismic Code (NGSC), which evolved into the Greek Code for Seismic Resistant Structures (EAK 2000). The overall philosophy of this code is to make structures tolerable to minor and repairable damages to the structural elements, minimizing damages for lower-intensity earthquakes. New parameters were introduced, such as the use and significance of a structure to determine its functionality after the event. The seismic design acceleration, $R_d(T)$, (equivalent to the coefficient, ε, of previous codes) depends on several factors. These factors are the expected ground acceleration, A, the seismic hazard zone (three zones I, II, III), the natural period of the structure, T, the ductility factor, q (material, over-strength, static system), the importance factor, γ_1 (four categories S1, S2, S3, S4), and the foundation factor, θ. The design spectrum is formed based on these factors, and the seismic design acceleration, $R_d(T)$, is calculated. The modern methods for calculating the seismic intensity due to seismic actions are the following : (a) the dynamic spectral method, which is generally applied in all cases; (b) the simplified spectral method (equivalent static), which is applied under conditions depending on the regularity of the building, the number of floors, the importance, and the seismic zone, and (c) in exceptional cases, additional checks are allowed, and for safety reasons, other calculation methods such as linear or nonlinear analysis with time integration are permitted.

1.2 Control theory: historical elements and basic principles

Automatic control places its roots far behind in the depths of history. One of the first ancient automatic control systems was the water clock invented by the Greek engineer Ctesibius, who served the king of Egypt, Ptolemy V, in Alexandria. The subsequent encounter with automatic control systems is placed three centuries later by Hero of Alexandria. His book ‘’Pneumatica’’ describes many of his control devices in detail. The most famous of his works is the automatic opening system of the temple door. This system was designed to automatically open the temple gate when a fire was lit in the temple and close it when it went out.

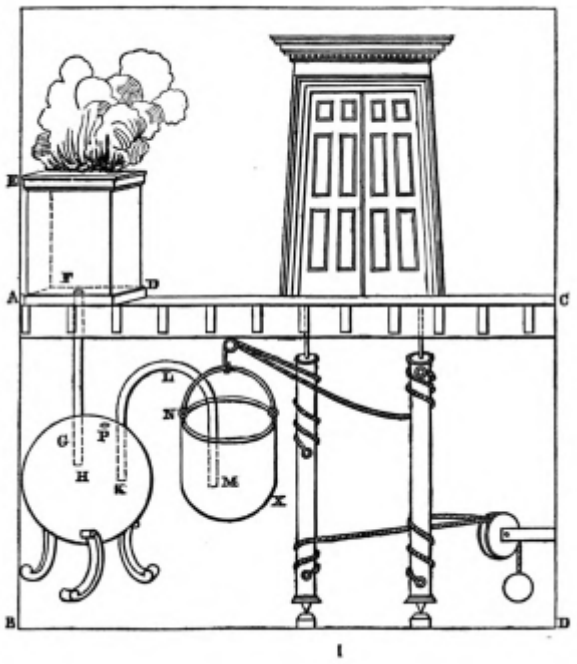

Figure 1. Ancient automatic control system: Hero's automatic temple doors (Lowinger 2017)

The operational sequence of the system is the following: the fire heated the air under the altar, and the hot air pushed water from container 1 to container 2. The containers were suspended with ropes, which were properly wound in a mechanism with a counterweight W. When container 2 was empty, this mechanism under the weight W kept the gate closed. When enough water from container 1 entered container 2, it descended, causing the mechanism with the ropes to open the gate. When the fire extinguished, the water from container 2 returned to container 1, and container 2 rose, closing the gate. This regulator was used to impress the faithful, as the automation system was hidden in the ground. The next major encounter of automatic control systems is placed after 800 years in the 9th century in the Arabian Peninsula. The author of the book "Kitab al hiyal" ("On Ingenious Devices"), describes a regulator with a flow system. His name remains unknown, and as a result he is called "Pseudo-Archimedes''. In the 13th century the only work available is by Ibn-Sacati and Al-Jazari. After the 13th century the documents seize with no relevant source dating back to the Middle-Ages or the Renaissance. The next reference of automation is by William Salmon in 18th century. In 1758, the steam engine was built. This engine used a valve to regulate the water level in the boiler. In 1784, Sutton Thomas Wood created the new automatic control engine, based on the ideas of Hero.

One of the most famous automatic control devices is the thermostat. It has its roots in the German engineer Cornilius Drebbel, who is the one who invented it, according to Francis Bacon. The invention itself was an accident. Drebbel thought that if he could maintain a stable temperature in a process for an extended period, he could transform common metals into gold.

The development of automation from 1869 is characterized as a time of progress without any mathematical basis. This situation changed in 1868 with Maxwell and in 1877 with Wischnegradnsky. Maxwell worked around the stability of Watt's governor, and Wischnegradnsky

followed with a more detailed analysis of third-order stability. In 1922, Minorsky applied non-linear control system principles in his study of automatic ship steering.

In the 20th century, many devices, such as pyrometers, voltmeters, and memory, were developed. Automation was introduced into the American steel industry in 1900. In 1912, Henry Ford, using the mass production principle, achieved 1000 cars per day when cars were considered a luxury.

In the 1920s and 1930s, significant work was done regarding theoretical and practical findings by Minorsky, Hazen, Nyquist, and Black. The year 1934 is a significant milestone in the history of automatic control with the publication of Harry Nyquist's article titled "Theory of Servomechanisms" in the "Journal of the Franklin Institute." The term "servant" declares that these machines were designed to serve humans. The American Society of Mechanical Engineers states: "A feedback control system is a system that seeks to maintain a predetermined relationship of one variable of the system to another using their difference as a means of control."

A system is a set of elements that are appropriately connected to perform a task. A system must be given a stimulus to perform a task, as shown below in Fig.2.

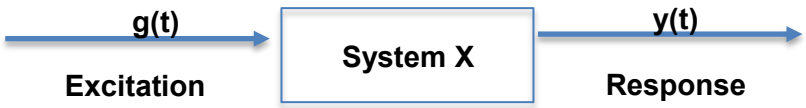

Figure 2. Control system, excitation and response

Where X denotes the system, g(t) is the excitation which connects with the response y(t) with the following equation:

$$y(t) = X(g(t)) \quad (1)$$

An automatic control system is a system where each element is connected in a predetermined, desirable way.

Designing an automatic control system is a problem that, given the system **X** and the desirable behaviour **ydes(t)**, an excitation **g(t)** is demanded in order for the response **y(t)** to be desirable and predetermined. In an automatic control system, the input **g(t)** is not the product of a signal generator but the output of an additional signal **T1**, which is usually called a regulator.

Automatic control systems can be classified into open-loop and closed-loop systems. An open-loop is a system where the input **g(t)** is not a function of the output **y(t)**. A closed-loop system is a system where the input a(t) is a function of the output y(t). This is achieved by measuring the output y(t), comparing it with a desired output, and driving the difference to the system's input. This process is known as feedback.

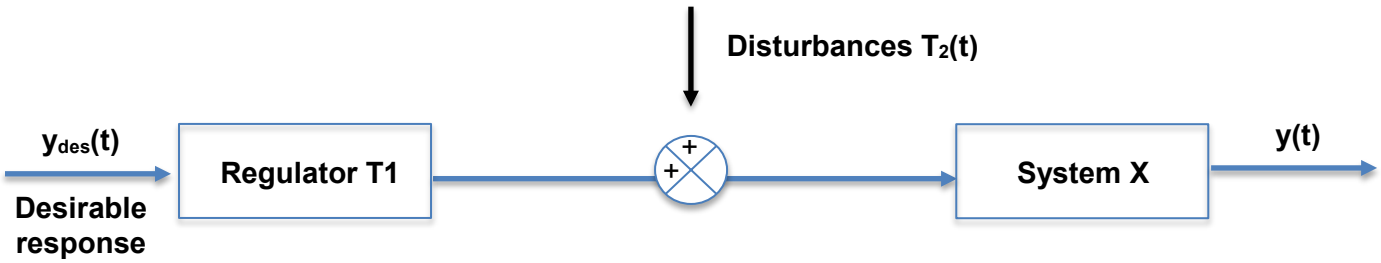

Figure 3. Open-loop control system with disturbances

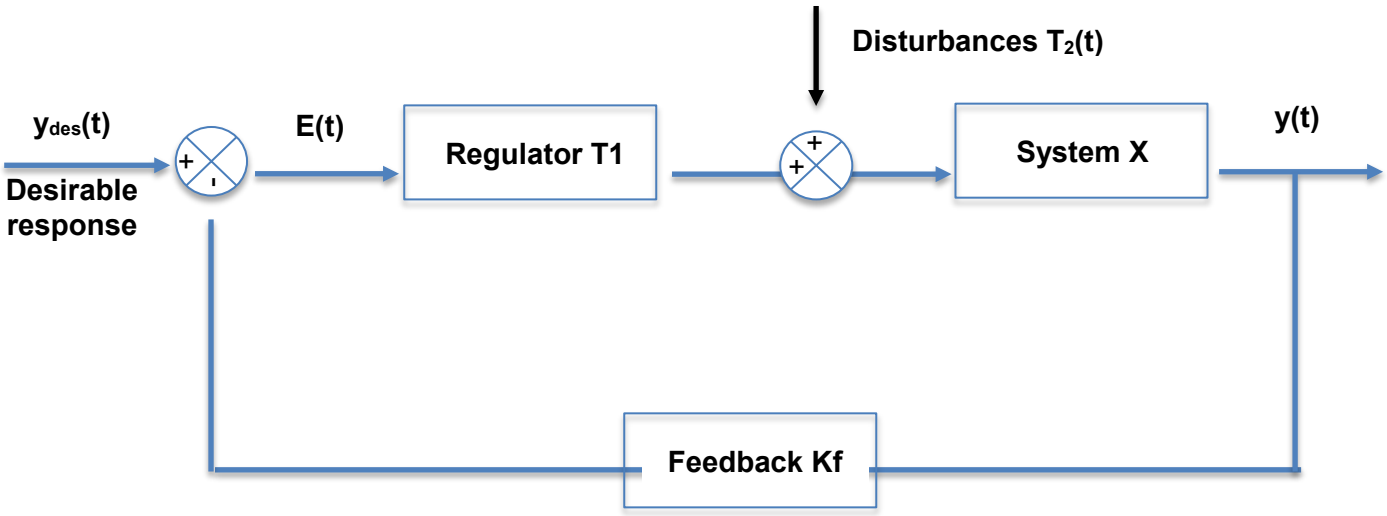

Figure 4. Closed-loop control system with disturbances

The output of the open-loop control system connects with the input with the following equation:

$$y(t) = X(g(t) + T_2(t)) \quad (1)$$

Where T2(t) denote the system disturbances. However, because:

$$g(t) = T_1\left(y_{des}(t)\right) \tag{2}$$

Eq. 2 becomes,

$$y(t) = XT_1\left((y_{des}(t)) + T_2(t)\right) \tag{3}$$

For a closed-loop system the equation that connects the input with the output is:

$$y(t) = X\left(T_1\left(E(t)\right) + T_2(t)\right) \tag{4}$$

Because of the feedback Eq. becomes:

$$E(t) = y_{des}(t) - K_f\, y(t) \tag{5}$$

If E(t) is replaced in the y(t), it becomes,

$$y(t) = X\left(T_1(y_{des}(t) - K_f\, y(t)) + T_2(t)\right) \tag{6}$$

This is a general perspective of feedback, open and closed loop systems. More can be found in both Greek and international literature. Some examples are Abdel-Rohman (1980), Ogata (1997), Housner et al (1997), Pnevmatikos et al. (2016), Pnevmatikos and Gantes (2014). Open and closed loop systems are implicated in structural control as open and closed loop controlled structures.

2 Structural control

2.1 Passive structural control

Passive structural control is applied in structures through devices that do not require power. The typical examples are base isolation, tuned mass dampers (TMD), tuned liquid dampers (TLD), metallic yield dampers, viscous fluid dampers, and friction dampers. The earthquake action minimizes the earthquake action using the structure's motion to dissipate energy to alter the dynamic properties of the structure (damping, natural frequencies) or to produce relative movement within the control device. Their advantages are that they require low maintenance and no requirement for a power supply. They also perform better in structures with large eigenperiod values. Their disadvantages are that they require a large amount of space relative to their performance and high installation cost. They operate by receiving dynamic excitations (wind, earthquake, etc.) and reducing the system's response in a one-way route. The operation is displayed below in (Fig.1).

Figure 5. Structure with passive energy dissipation device (PED)

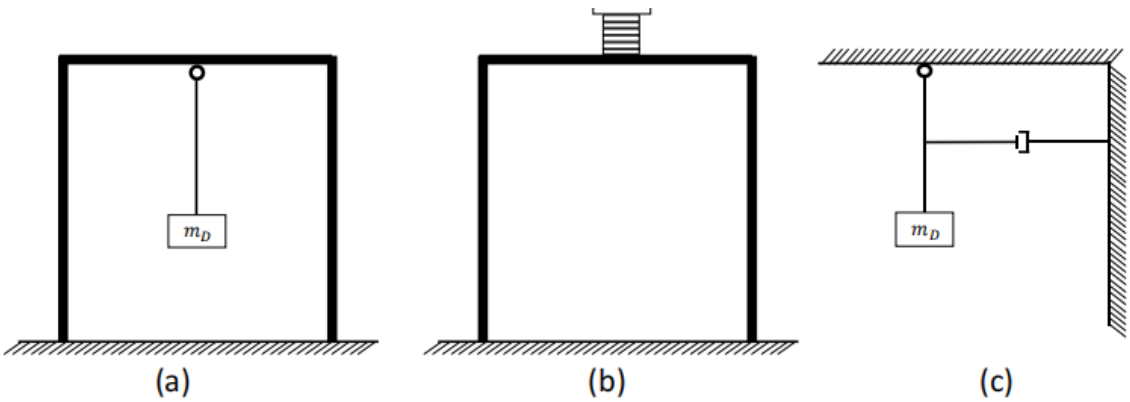

Figure 6. Types of TMDs : a) simple pendulum, b) mass on rubber bearings, c) pendulum with damper (Naveed Anwar 2016)

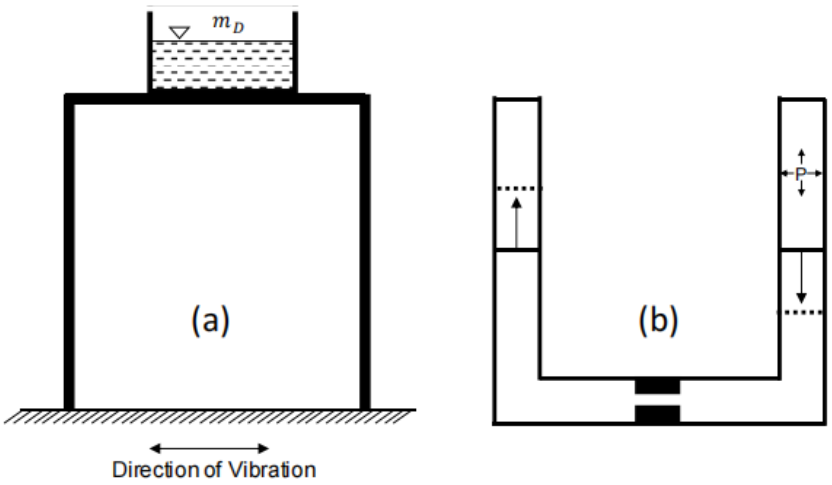

Figure 7. Types of TLDs : a) sloshing damper with meshes and rods, b) column damper with orifice (Naveed Anwar 2016)

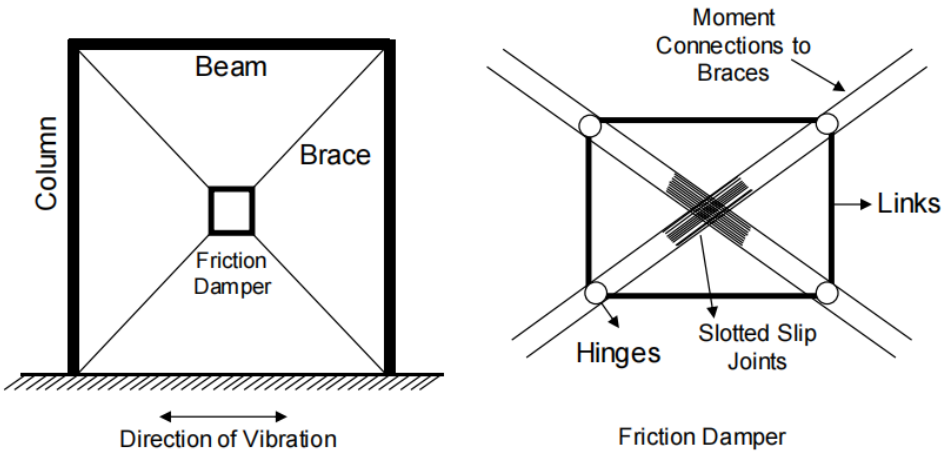

Figure 8. X-braced friction damper (Naveed Anwar 2016)

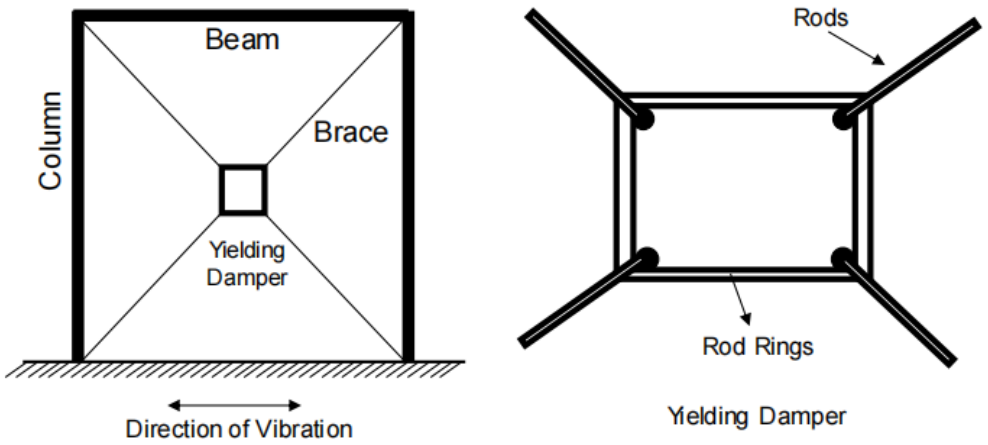

Figure 9. Metallic yield damper (Naveed Anwar 2016)

2.2 Active structural control

Active control algorithms were developed in the 1990s Soong (1990), Housner et al. (1997), Kobori et al. (1998), and Spencer et al. (1997). There are also other well-established algorithms in control engineering introduced by Yang (1975), Abdel-Rohman et al. (1980) sliding mode control Yang et al. (1995), H2 and H∞ Kose et al. (1995), Zacharenakis et al. (2001). As for structural applications, the best-fitted algorithm was described by Soong (1990). The structure is equipped with accelerometers on the lowest and the highest level. These sensors receive the excitation signal fed to the computer controller. In this phase, the control algorithms calculate the force needed to reduce the response quantities. The force is applied to the building, which responds. The sensors detect new displacements, velocities, and accelerations, which continue to feed the algorithm with the next part of the signal. The whole operation is displayed below in (Fig. 2).

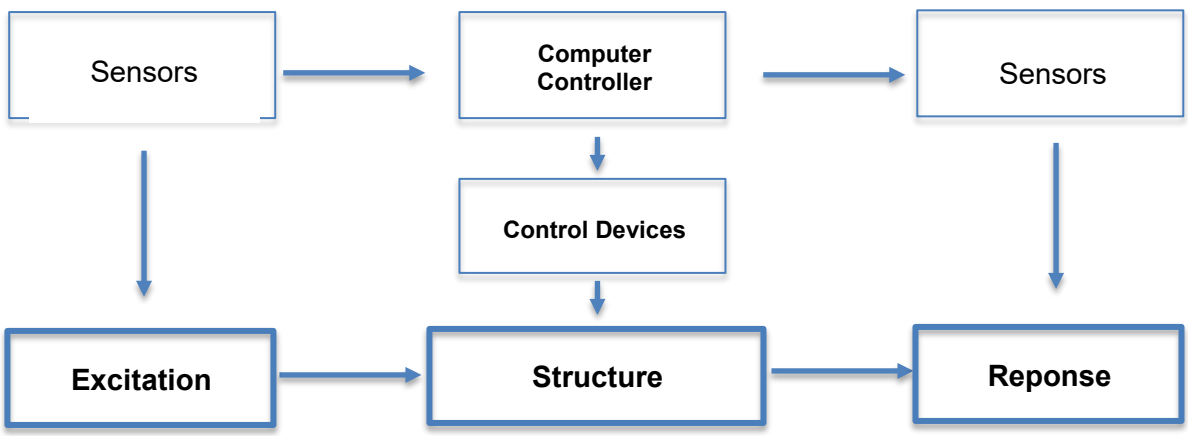

Figure 10. Structure with active control device

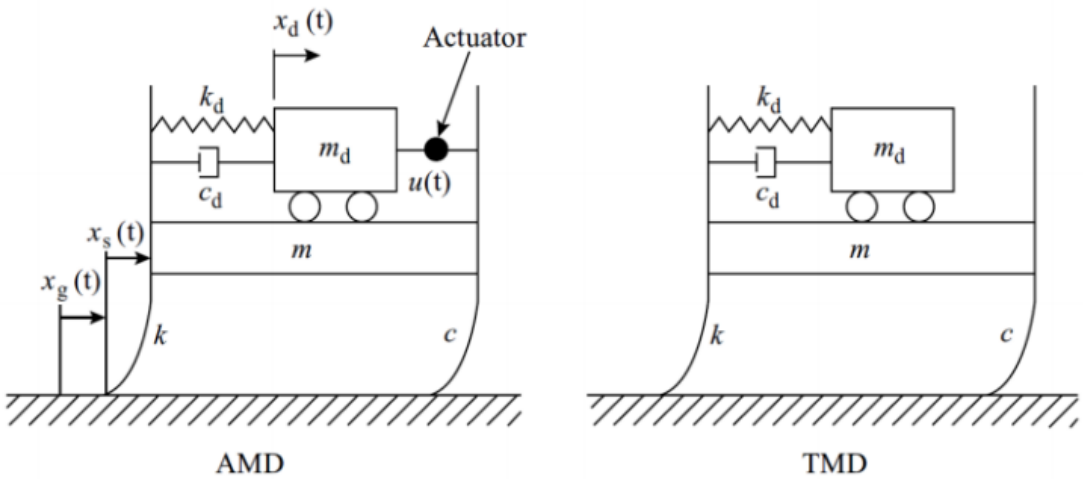

Figure 11. Comparison between structure equipped with AMD and TMD (Naveed Anwar 2016)

2.3 Semi-active control

Semi-active control is applied in structures by adapting active control devices to reduce the power supply requirement. The external power is not used to change the device's properties, such as damping or stiffness, and does not generate control force Symans et al. (1994). Semi-active control devices are not in place to provide energy to the controlled system. Thus, varying their properties reduces the system's response Housner et al. (1997). The significant difference from the active control devices is that the semi-active devices do not destabilize the structural system. In case of power failure, they do not require batteries since they function as passive devices Soong et al. (2002).

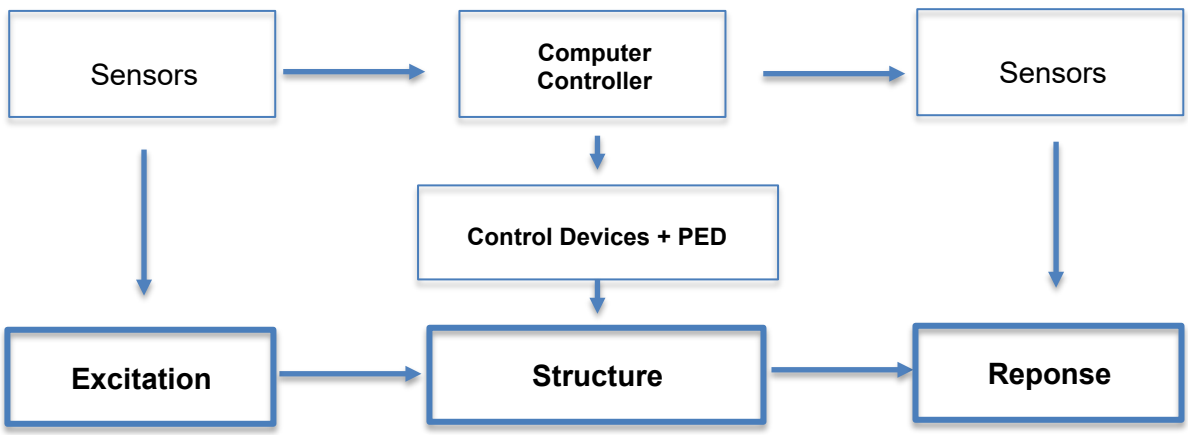

Figure 12. Structure with semi-active control devic

The most typical examples include variable orifice fluid dampers, controllable friction devices, variable stiffness devices, controllable liquid dampers, and controllable fluid dampers. To be more specific, a variable orifice fluid damper is a fluid damper that uses an electromechanically variable orifice to alter the resistance to the flow of a conventional hydraulic fluid, Feng et al. (1992) and Constantinou et al. (1993).

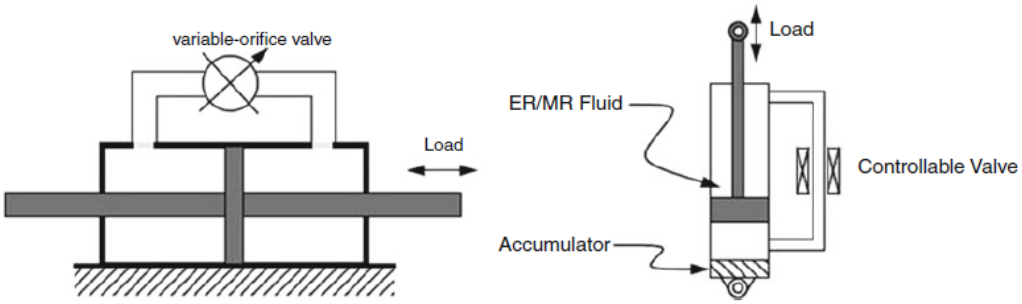

Figure 13. Variable-orifice damper and controllable fluid damper (Nikos Pnevmatikos 2014)

As for the semi-active controllable fluid devices consist of fluid dampers that can change the viscosity of their fluid. Electrorheological fluids (ER) and magnetorheological fluids (MR) are the two main categories. The MR fluids consist of magnetically polarized particles suspended in an oil medium. The ER fluids consist of dielectric polarizable fluids suspended in an oil medium.

Their primary ability is that they change from viscous fluids to semisolids with controllable yield strength in milliseconds; this is achieved by applying an electrical or magnetic field, respectively. Their simplicity and lack of complex parts make them reliable and easy to maintain. The first reference to ER and MR fluids can be found in Winslow (1947). The development of ER fluid dampers has been done by Ehrgott and Marsi (1992), Ehrgott and Marsi (1993), (Makris et al. (1995). Other significant work can be found in Spencer and Nagarajaiah (1997), Soong et al. (2002), (Spencer and Nagarajaiah (2003), Carlson JD et al. (1995), Dyke et al. (1996).

Other types of semi-active control devices use the so-called sloshing effect. This effect refers to the dynamic motion of a fluid column, reducing the structure's response. These dampers are the successors of passive-tuned sloshing dampers (TSD) and tuned liquid column dampers (TLCD). Both of them use a liquid in a sloshing tank, driven by the system's vibrations, to reduce the system's response. The effectiveness of passive systems is low. A semi-active device based on the passive TSD changes its natural frequencies to improve it. In semi-active devices based on a TLCD, a variable orifice is used within the liquid tank, or the cross-section of the sloshing tank is changed.

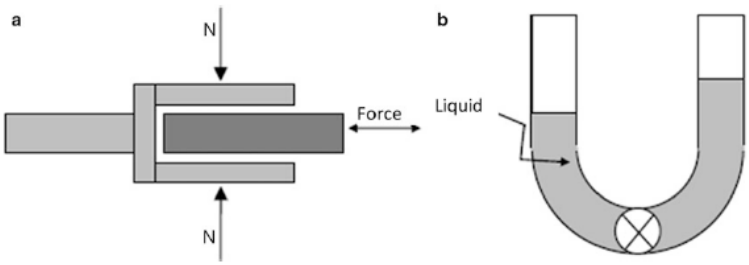

Figure 14. Friction semi-active device (a) Semi-active tuned liquid column damper (b) (Nikos Pnevmatikos 2014)

The similarity between TMDs and semi-active tuned mass dampers is something worth mentioning. The most significant difference is that the semi-active TMD can vary its level of damping. They are primarily applied in structures excited by wind loads.

Another semi-active TMD is the semi-active variable stiffness-tuned mass damper (SAIVS-TMD). Its main characteristic is the controllability of the stiffness. They perform similarly to active mass dampers but with significantly reduced energy consumption. The structure's stiffness and natural frequency modification to avoid resonant conditions have been studied by Kobori et al. (1993).

Semi-active variable stiffness-tuned mass dampers are installed in bracing systems, and by opening and closing, a valve allows the connection between the brace and the beam. This way, the structure's stiffness and natural frequency change, and the resonance with the earthquake excitation is avoided. They are highly efficient in energy consumption, and in case of power failure, the connection closes automatically, increasing the building's stiffness.

2.4 Hybrid control

The fundamental principle of hybrid control is the equal participation of active devices in passive systems or the opposite. The combinations aim to lower the forces required by active or semi-active systems. The most typical example is the hybrid mass damper (HMD). The HMD combines tuned mass dampers with active actuators. The structure responds passively along with the damper using the actuator force only to increase efficiency and robustness to changes in structural dynamic characteristics.

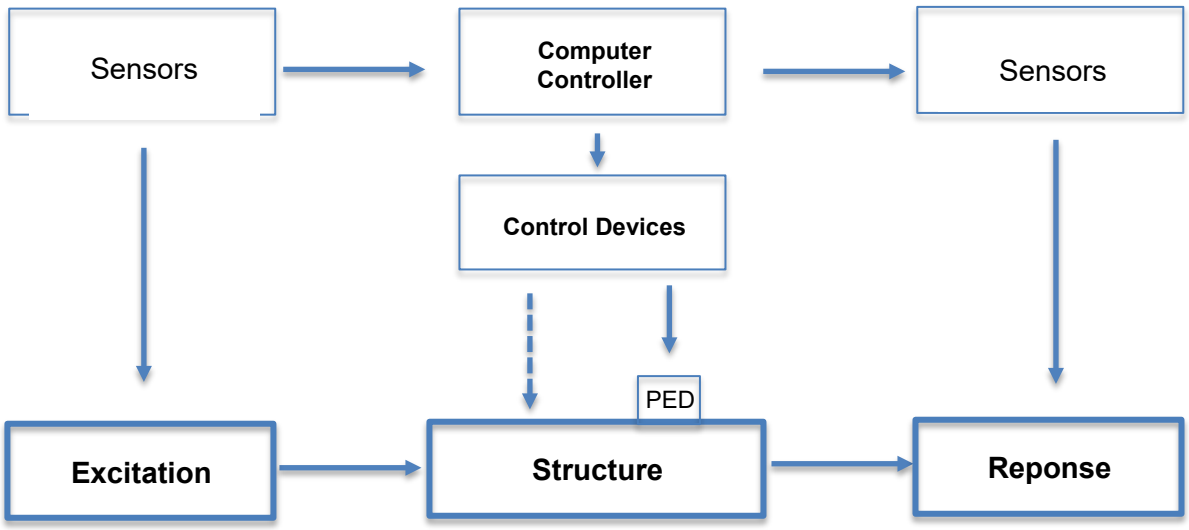

Figure 15. Structure with hybrid control device

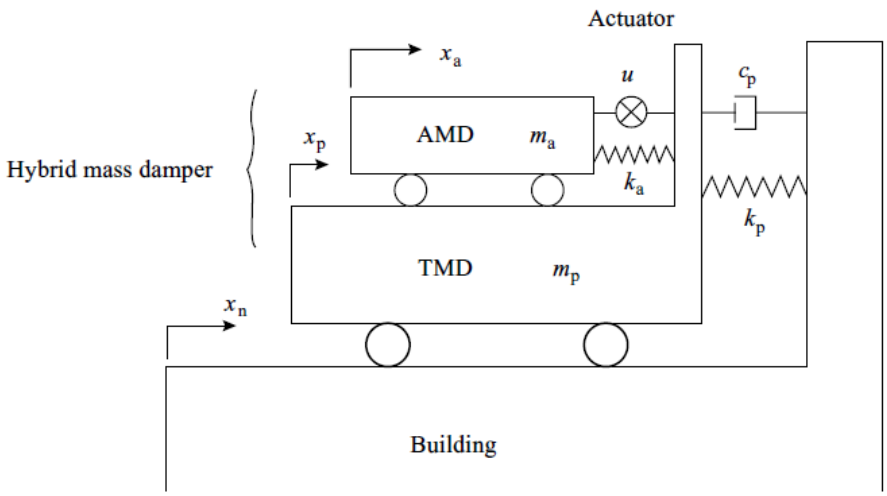

Figure 16. Model of a hybrid mass damper (Naveed Anwar 2016)

One example in the category of hybrid mass dampers is the active-passive composite tuned mass damper (APCTMD) created and studied by Ohrui et al. (1994), which has the name DUOX. As displayed below, the device layout consists of an active mass damper mounted on a tuned mass damper.

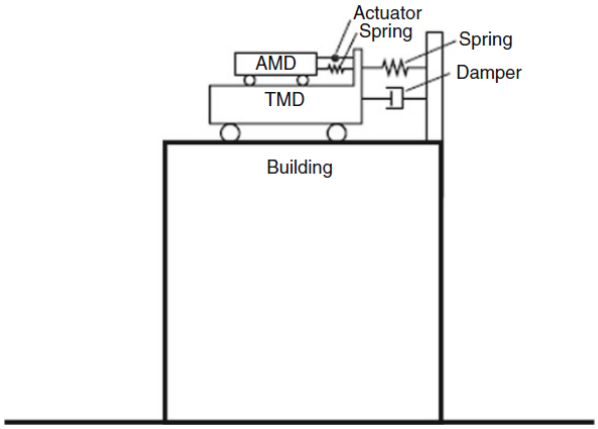

Figure 17. Simplified diagram of DUOX control system (Nikos Pnevmatikos 2014)

In the first stage, the mass of the active device is driven in the opposite direction of the passive device, resulting in the magnification of the passive device's motion. After the building deformation stops, the AMD is used to suppress any useless motion of the TMD.

In the case of base isolation systems, they are passive systems. Therefore, by adding active devices, a higher level of performance can be achieved with minimum cost. This system is often called hybrid seismic isolation, consisting of active or semi-active devices introduced in base-isolated structures.

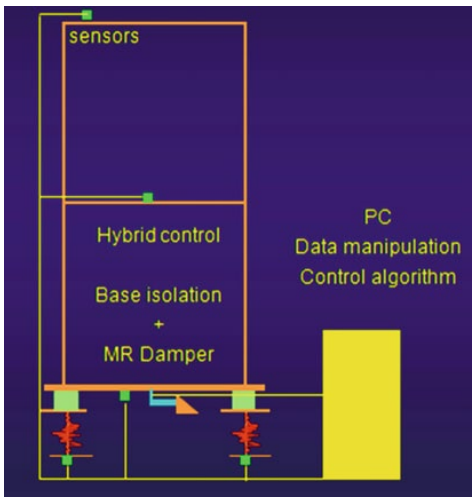

Figure 18. Hybrid control system (Nikos Pnevmatikos 2014)

Base isolation reduces inter-story drifts and structural accelerations, increasing base displacement. Hence, an active or semi-active device is needed. The semi-active friction-controllable fluid bearing can be used parallel to the base isolation system Feng et al. (1992) and Sriram et al. (2003).

The first hybrid control strategy was implemented in the Ando Nishikicho Building in Tokyo, Japan, in 1993. The control system acts as a passive device in moderate earthquakes and strong winds. In

the case of stronger earthquakes or dynamic excitations, where the ground excitation is spread over a wider frequency band, and the first mode of vibration is not considered dominant, the actuator is activated, reducing the response quantities due to higher modes. Another application is the one of the USC University Hospital. Linear bearings passively control the buildings, providing lateral stiffness and controlling natural vibration period and hysteretic damping. As for the active control, viscous damping devices were chosen, providing velocity-dependent damping, which controls the overall building displacements. The Kansai International Airport in Osaka, Japan; the Mitsubishi Heavy Industry in Yokohama, Japan; and the RIHGA Royal Hotel in Hiroshima, Japan, are famous applications of hybrid mass dampers.

Lin et al. (2007) Extensive experimental tests were conducted on a mass equipped with a hybrid-controlled base isolation system. The system consisted of a rolling pendulum (RPS) and a 20-KN magnetorheological (MR) damper. The system was subjected to far-fault and near-fault earthquakes on a giant shake table. The results showed that by combining rolling pendulum systems with MR dampers, robust vibration control can be provided for large civil engineering structures that need protection from a wide range of seismic events.

Design and implementation of active, semi-active, and hybrid systems can also be found in the work of Chu et al. (2005) and Yi et al. (2001).

3 Modeling

3.1 Continuous and Discrete Control

The equations of motion of a controlled structural system with n degrees of freedom subjected to an earthquake excitation ag in state space are described below.

$$\mathbf{M}\ddot{\mathbf{U}}(t)+\mathbf{C}\dot{\mathbf{U}}(t)+\mathbf{K}\mathbf{U}(t)=\text{-}\mathbf{M}\mathbf{E}\,a_g(t)+\mathbf{E}_f\mathbf{F}(t) \tag{7}$$

Where **M, C, and K** denote the structure's mass damping and stiffness matrices, respectively**, E, Ef** is the location matrix for the earthquake and the control forces on the structure, and F(t) is the control force matrix applied to the structure.

In state space approach Eq.1 can be written as below:

$$\dot{\mathbf{X}}(t)=\mathbf{A}\mathbf{X}(t)+\mathbf{B}_g a_g(t)+\mathbf{B}_f\mathbf{F}(t) \tag{8}$$

$$\mathbf{Y}(t)=\mathbf{C}\mathbf{X}(t)+\mathbf{D}\mathbf{F}(t)+\mathbf{v}$$

The matrices **X, A, B_g, B_f** are given by

$$\mathbf{B}_g=\begin{bmatrix}\mathbf{O}\\ -\mathbf{E}\end{bmatrix}_{2nx1},\mathbf{B}_f=\begin{bmatrix}\mathbf{O}\\ \mathbf{M}^{-1}\mathbf{E}_f\end{bmatrix}_{2nx1} \tag{9}$$

$$\mathbf{X}=\begin{bmatrix}\mathbf{U}\\ \dot{\mathbf{U}}\end{bmatrix}_{2nx1},\ \mathbf{A}=\begin{bmatrix}\mathbf{O} & \mathbf{I}\\ -\mathbf{M}^{-1}\mathbf{K} & -\mathbf{M}^{-1}\mathbf{C}\end{bmatrix}_{2nx2n}$$

The matrices **Y, C, D**, and **v** are the output states, the output matrix, the feed-forward control force matrix, and the noise matrix. Matrices **C and D** are equal to zero in case the output variables of the system are the same as the states and no control forces are applied to the system. The noise matrix deflects the characteristics of the sensor (accelerometer, etc.) that are used to measure the system's response. The above equation can be solved by any numerical technique for differential equations, like an explicit Runge–Kutta formula, the Dormand–Prince pair, Bogacki–Shampine, and Adams–Bashforth–Moulton PECE solver Pnevmatikos and Gantes (2014).

3.2 Linear and Nonlinear Control

Dynamic loads create changes in the mechanical properties of the materials. As a result, the stiffness matrix is changed, and the differential equation becomes non-linear:

$$\mathbf{M}\ddot{\mathbf{U}}(t)+\mathbf{C}\dot{\mathbf{U}}(t)+\mathbf{F}s(\mathbf{U}(t))=\text{-}\mathbf{M}\mathbf{E}\,a_g(t)+\mathbf{E}_f\,sat\,\mathbf{F}(t-t_d) \qquad (10)$$

The nonlinearity originates from the structure and is described as material nonlinearity. The equation of motion is formulated in the deformed configuration considering the structure's flexibility and large displacements, so it becomes non-linear. The origin of the nonlinearity is from the structure. Eq.4 describes it as geometric nonlinearity.

So, there are two cases. In the first case, the control force F is a linear function of the response. Thus, the equation of motion is a linear differential equation. In the second case, the control force F is a non-linear response function; thus, the equation of motion is a non-linear function of the response. The nonlinearity originates from the control force F.

3.3 Time delay – Saturation Capacity

Time delay and saturation capacity are two issues that appear during practical application. Time delay refers to the time it takes the algorithm and the overall system to calculate the control force. In contrast, the saturation capacity refers to the mechanical capability of the actuator. Both come into consideration by solving the differential equation as a delay differential equation with saturation effects. It is essential to consider these two parameters during the design process. This way, the modelling and reliability of the system will be more accurate.

The equation of motion of a controlled structural system considering time delay and saturation becomes

$$\mathbf{M}\ddot{\mathbf{U}}(t)+\mathbf{C}\dot{\mathbf{U}}(t)+\mathbf{F}s(\mathbf{U}(t))=\text{-}\mathbf{M}\mathbf{E}\,a_g(t)+\mathbf{E}_f\,sat\,\mathbf{F}(t-t_d) \qquad (11)$$

satF is the saturated control force matrix which is applied to the structure with time delay t_d and is given as

$$sat\mathbf{F}(t-td)=\begin{cases}\mathbf{F}(t-t_d) & |\mathbf{F}(t-t_d)<\mathbf{F}\,\text{allowable}\\ \mathbf{F}\,\text{allowable} & |\mathbf{F}(t-t)>\mathbf{F}\,\text{allowable}\end{cases} \qquad (12)$$

$\mathbf{F}_{\text{allowable}}$ is the maximum capacity of the control device. In state space approach the equation of motion can be written as follows:

$$\dot{\mathbf{X}}(t) = \mathbf{A}\mathbf{X}(t) + \mathbf{B}_g a_g(t) + \mathbf{B}_f sat\mathbf{F}(t- t_d) \quad (13)$$
$$\dot{\mathbf{Y}}(t) = \mathbf{C}\mathbf{X}(t) + \mathbf{D}\mathbf{F}(t- t_d) + \mathbf{v}$$

Eq.7 can be solved using the following tranformatrion,

$$\mathbf{Z}(t) = \mathbf{X}(t) + \int e^{-\mathbf{A}(\eta+td)}\mathbf{B}\,f\,\mathbf{E}(t+\eta)\,d\eta \quad (14)$$

and,

$$\dot{\mathbf{Z}}(t) = \mathbf{A}\mathbf{Z}(t) + \mathbf{B}\,ga_g(t) + \mathbf{B}(\mathbf{A})\mathbf{F}(t) \quad (15)$$
$$\mathbf{B}(\mathbf{A}) = e^{-\mathbf{A}t_d}\,\mathbf{B}\,f$$

The control process is about measuring response data, computing control forces through an appropriate algorithm, transmitting data and signals to actuators, and activating the actuators to a specified level of force. Thus, time delay cannot be avoided. In a single-degree-of-freedom system, much work is done Connor (2003). Obtaining these results following this approach is very difficult in multiple degrees of freedom. However, many attempts have been made by Casciati et al. (2006) to solve numerically delayed differential equations. All this work shows the importance of time delay in control applications in structures.

Actuation saturation is overcoming the device's peak capacity by the required control force calculated by the algorithm. Most algorithms are linear. This is why there is no limit to the calculated control force. Saturation can lead to a reduction in the efficiency of the system. In most cases, the solution in this case is the placement of multiple devices, mainly in case of active mass damper application, in parallel. In combination, these two issues can drive the controlled structure to become unstable and behave worse than before. Pnevmatikos (2011) They have studied a combination of these issues and proposed limits for a pair of time delay and saturation capacities that can be used in the design process of controlled structures.

3.4 Controllability – Observability

The controllability of a system refers to the number of control positions and degrees of freedom of the structure. Precisely, these two values must be equal for the system to be fully controlled. However, this means the structure will behave as one of infinite stiffness, and the relative displacements between the floors will be zero. In reality, control positions are fewer than the degrees of freedom of a building. This way, the best we can do is to investigate the appropriate locations of the control forces so that the response can be reduced to a satisfactory level.

A system is said to be observable at time t0 if, with the system in state x(t0), it is possible to determine this state by observing the output over a finite time interval Ogata (1997). This is the case, as mentioned above, that the structure behaves as a rigid body and full-state feedback is achieved. This is called feedback without an observer.

4 Control strategies and algorithms

4.1 Introduction

Control algorithms are no more than different ways to solve the state space differential equation mentioned above. Their goal is to calculate the control force F through the feedback matrix. The most typical examples are optimal control, LQR or LQG, pole assignment, sliding mode control, H2 and H∞, fuzzy control, and many others. For structural application, these algorithms are best described by Soong (1990) and Casciati et al. (2006).

4.2 Pole placement algorithm

Pole placement refers to the eigenvalues of matrix **A** of Eq.8 to desirable locations in a plane of real and imaginary numbers. For this algorithm, eigenmodes and eigenperiods of the uncontrolled system need to be calculated to solve the following eigenvalue problem:

$$\left[\mathbf{K}-\boldsymbol{\omega}^2\mathbf{M}\right]_{nxn}\boldsymbol{\Phi}=0 \qquad \mathbf{T}_i=\frac{2\pi}{\boldsymbol{\omega}_i},\ \mathbf{f}_i=\frac{\boldsymbol{\omega}_i}{2\pi},\ \mathbf{i}=\mathbf{0},\ldots,\mathbf{n}-\mathbf{1} \qquad \begin{aligned}\mathbf{C}_n&=\boldsymbol{\Phi}_n^T\mathbf{C}\boldsymbol{\Phi}_n\\ \mathbf{M}_n&=\boldsymbol{\Phi}_n^T\mathbf{M}\boldsymbol{\Phi}_n\\ \xi_i&=2\mathbf{C}_n\mathbf{M}_n\omega_n\end{aligned} \tag{16}$$

The eigenvalues of the system are obtained directly from the eigenvalues of matrix **A**, as indicated by the equation:

$$\det\left[\lambda\mathbf{I}-\mathbf{A}\right]=0\rightarrow\lambda_i \qquad \lambda_i=-2\pi f_i\xi_i\pm j2\pi f_i\sqrt{1-\xi_i^2} \tag{17}$$

It is assumed that the control force **F** is determined by linear state feedback:

$$\mathbf{F}=-\mathbf{G}_1\mathbf{U}-\mathbf{G}_2\dot{\mathbf{U}}=-\mathbf{G}\mathbf{X} \tag{18}$$

G is the gain matrix which is calculated according to the desired eigenvalues (poles) of the controlled system. Replacing the force **F** into Eq.8, the closed loop (controlled) system becomes:

$$\dot{\mathbf{X}}=\left(\mathbf{A}-\mathbf{B}_f\mathbf{G}\right)\mathbf{X}+\mathbf{B}_g a_g \tag{19}$$

The new eigenvalues λ_{ic} of the controlled system satisfy the following equation:

$$\det\left[\lambda\mathbf{I}+\mathbf{B}_{\mathrm{f}}\mathbf{G}-\mathbf{A}\right]=0 \tag{20}$$

The state feedback design selects the gain matrix **G** so that the roots (eigenvalues) of Eq.14 are at the desired locations. The desired eigenvalues λic of the controlled system also satisfy the equation:

$$\left(\lambda-\lambda_{1c}\right)\left(\lambda-\lambda_{2c}\right)\ldots\left(\lambda-\lambda_{nc}\right)=0 \tag{21}$$

Choosing the gain matrix **G** in such a way that Eq.14 equals Eq.15 will force the system to have the desired eigenvalues. This procedure is not applicable in higher degree of freedom systems where other suggestions and techniques have been mentioned by Kautsky and Nichols (1985) along with Laub and Wette (1984).

4.3 Pole placement in structures

In structures, a pole placement algorithm is used to intervene in the system to achieve the desired dynamic characteristics, denoted as λic, in order to satisfy the design requirements. The question arises: what will be the desired dynamic characteristics for the control system, and how will these be calculated through automated and systematic processes suitable for computer programming. A generic view regarding this question is that the desired dynamic characteristics should be such that they do not correlate structure with the dynamic loading conditions, as mentioned by Pnevmatikos (2007). In addition, since the loading conditions vary each time, the dynamic characteristics of the controlled system should be calculated through a process that relies on the specific loading characteristics and is applied during the imposition of the load on the structure.

To begin with, from the researcher's perspective, the successful application of the pole placement algorithm requires the proper selection of the eigenvalues-poles of the controlled structure. Pnevmatikos (2007), focused on establishing a systematic method for selecting the poles of the controlled system suitable for real-time computation. The dynamic characteristics of the signal that excites the structure are the fundamental principle for calculating the poles of the controlled system. The pole selection process is initially based on the spectrum of the incoming signal, then on mapping the spectrum onto the complex plane, and finally on determining the positions of the poles based on specific rules. The process is automated and repeated for each successive segment of the input excitation. Each input signal segment is analysed using the Fast Fourier Transform (FFT) of wavelet analysis, and its frequency content is identified. The next stage consists of the calculation of a window of significant frequencies. The eigenfrequencies of the controlled system need to be outside of this window. If *fL* and *fH* are the lowest and highest frequencies of the window, then the eigenfrequencies λic of the controlled system should be outside the interval [*fL, fH*].

There is also the case where the structure has its eigenfrequencies within the window of significant frequencies yet avoids resonance. This can be seen when the window of significant frequencies has multiple 'valleys.' The next step involves detecting these regions and determining when to place the poles in such areas. The adaptation of the algorithm is based on different scenarios and makes decisions based on real-time seismic excitation. The structure's safety is ensured by shifting its eigenfrequencies outside the window of significant frequencies. However, in shifting the eigenfrequencies, we must be made aware of whether the earthquake is nearby or the specific soil conditions beneath the structure.

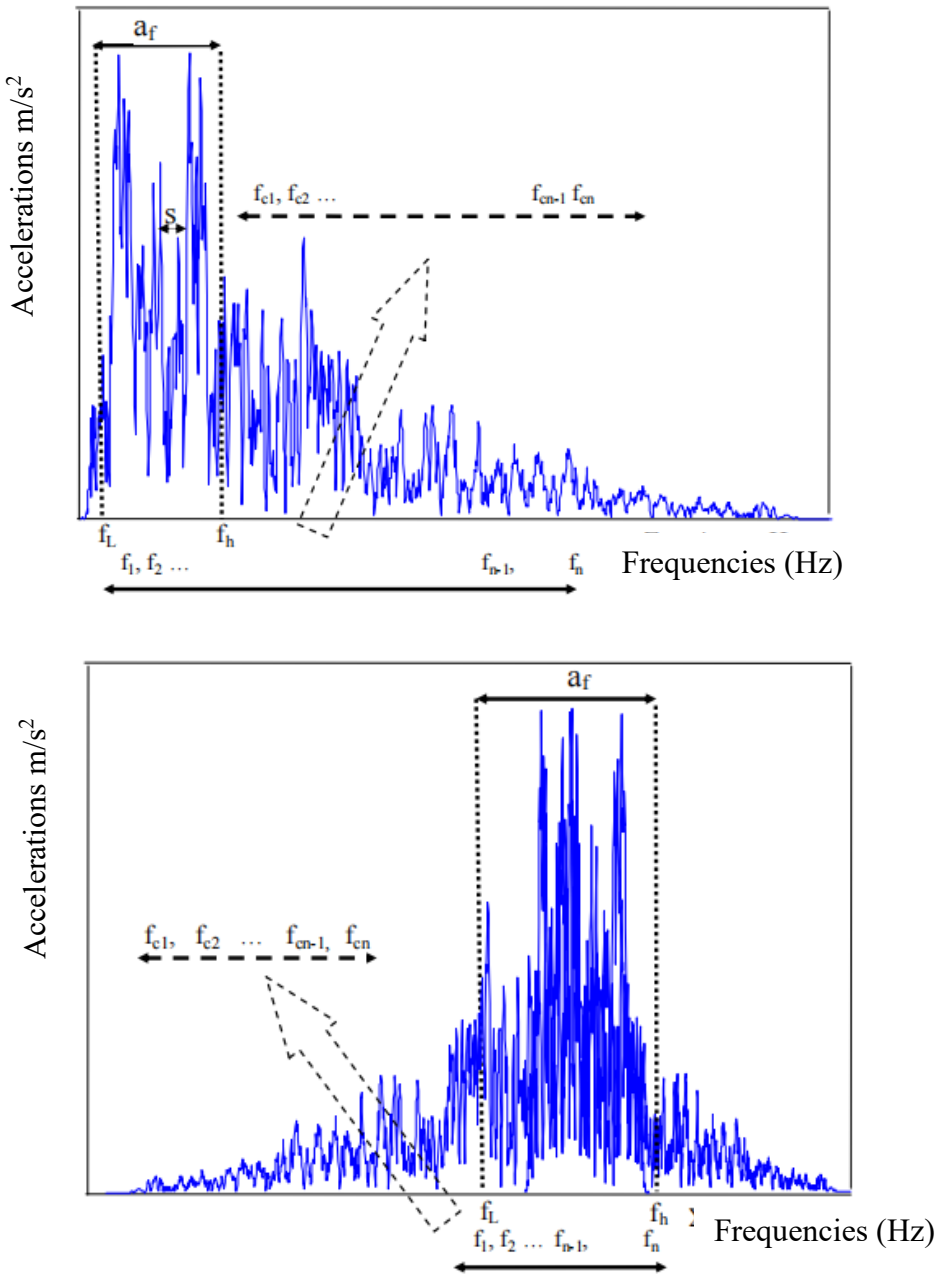

Figure 19. The frequency range of the window of significant seismic frequencies is defined by the lower frequency f_L and the higher frequency f_H. The initial eigenfrequencies of the system, denoted as 1,2,…,f_1,f_2,…,fn, are compared with the new positions of the eigenfrequencies,1,2,…,f_{c1},f_{c2},…,fcn,

under two different scenarios: low-frequency excitation (distant earthquake) and high-frequency excitation (nearby earthquake) (Pnevmatikos 2007).

This process allows us to avoid resonance. Nonetheless, an excitation may not resonate with the system but push it beyond its elastic range, causing damage. Therefore, besides avoiding resonance, control should continue to protect the structure. In this case, the only value that can be altered to reduce the structure's displacements is the equivalent damping ratio ζi. By changing the damping ratio, we alter the eigenvalues (poles) of the controlled system, reducing its response even when it is not resonating with the excitation. In the frequency domain, while there is a clear picture of the eigenfrequencies of the structure concerning the excitation frequencies and the positions of the eigenfrequencies of the controlled structure, there is no clear image of the influence of the damping ratio on shaping the eigenfrequencies of the controlled structure.

Moreover, since the eigenvalues are complex numbers, their real and imaginary parts are influenced by frequency and damping ratio. Thus, we can represent the excitation and the structure on the complex plane through suitable transformations. With a systematic procedure, we can choose the eigenfrequencies (poles) of the controlled structure to avoid resonance and have satisfactory damping ratios, ensuring that the structure adequately withstands the seismic excitation imposed upon it.

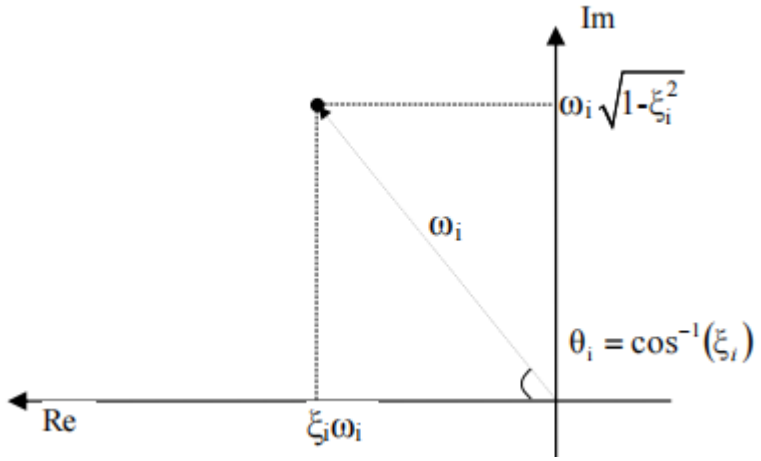

Figure 20. The relationship between the position of the pole in the complex plane and the dynamic characteristics (natural frequency, damping) of the structure is a crucial aspect in control theory.

Next, the steps of transforming the excitation to the complex plane are described below. At first, a Fast Fourier Transformation is conducted, and the frequency content is identified. In the case of a harmonic excitation, only one frequency is calculated, while in the case of seismic excitation, the FFT process yields multiple frequencies. Subsequently, based on the spectrum frequencies, circles are plotted in the complex plane with their centre at the origin and radii equal to the selected frequencies. All points on each of these circles are equidistant from the origin and correspond to the same natural frequency. In the case of harmonic excitation, a single circle is plotted, while in the case of seismic excitation, several circles are plotted. The process of transforming the excitation to the complex plane for harmonic and seismic excitation is illustrated below in Fig.21.

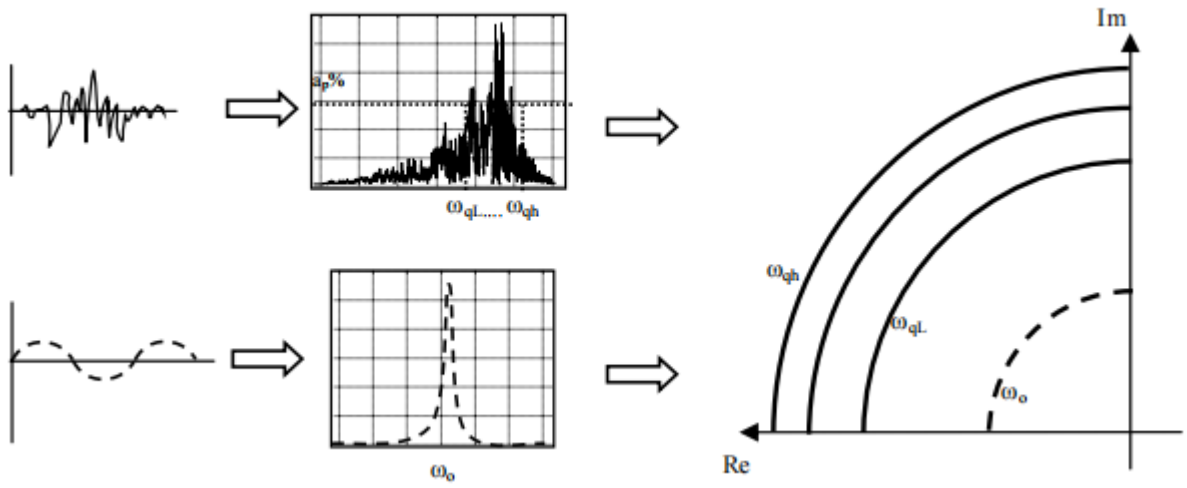

Figure 21. Transformation of harmonic and seismic excitation to the complex plane (Pnevmatikos 2007)

The procedure for calculating the poles goes as follows. The window of significant frequencies in the signal spectrum is initially transformed onto the complex plane. An initial signal segment is analyzed, and its spectrum is determined. Frequencies in the signal that need to be avoided are then selected based on their participation percentage in the spectrum and the signal's power. Circles are created in the complex plane, centred at the origin, with radii equal to the selected frequencies. All points on each of these circles are equidistant from the origin and correspond to the same natural frequency. Therefore, each point on the circle should be avoided as a possible pole position for the controlled structure to prevent resonance with the corresponding frequency of the seismic excitation. Next, a zone is defined inside and outside of each circle, known as the unsafe zone. After describing the seismic excitation and the significant frequencies in the complex plane, the poles of the initial structure are placed in the complex plane. The initial structure's natural frequencies and damping ratios, required to calculate the poles, can be obtained either computationally by solving an eigenvalue problem using the mass matrix M, damping matrix C, and stiffness matrix K or experimentally from a structural monitoring system. This way, Pnevmatikos (2007) suggested a computerized way of pole placing that is applied better in structures.

4.4 Linear Quadratic Regulator (LQR)

The equation of motion of a controlled structural system with n degrees of freedom subjected to an earthquake excitation ag in state space is described in Eq.1. We consider the optimal regulator problem that, given the system equation (Ogata 1997),

$$\dot{\mathbf{X}} = \mathbf{A}\mathbf{X} + \mathbf{B}u \tag{22}$$

the matric G of the optimal control vector is determined by,

$$\mathbf{F(t) = - Gx(t)} \tag{23}$$

to minimize the performance index,

$$\mathbf{J} = \int_0^\infty (\mathbf{x * Qx + F * RF})\ \mathrm{dt} \tag{24}$$

The reduced matrix Riccati equation that is obtained after the minimization of **J** is,

$$\mathbf{A * P + PA - PBR - 1\ B * P + Q = 0} \tag{25}$$

and the equation of the optimal matrix G is,

$$\mathbf{G = T - 1(T*) - 1\ B * P = R - 1\ B * P} \tag{26}$$

The matrix **G** is obtained by solving Eq.26 for the matrix **P** and substituting it for Eq.25. This method shows how to calculate the control force **F** using the linear quadratic regulator algorithm Ogata (1997). Other ways through algorithms to calculate it are described in Kautsky and Nichols (1985), Laub and Wette (1984).

4.5 Fuzzy logic control

Fuzzy logic, introduced by Zadeh (1965), applies fuzzy logic in control theory. It is similar to the human brain in dealing with uncertainty, vagueness and imprecision. The difference with Boolean logic is that the first determines whether an argument belongs to some set. In contrast, fuzzy logic considers the idea of partial truths and determines the degree of membership of an argument to a fuzzy set.

In fuzzy control, fuzzy rules are defined actions based on the measured structure's responses. The advantages of this type of controller are :

1. the simple algorithms,
2. no need for information on structural and vibration characteristics and
3. a robust system in terms of performance and implementation.

In fuzzy control, the controlled uses experience instead of differential equations to determine control actions. It uses close loops in the format of IF….THEN statements, which relate to input variables to the control actions. At first, all the response quantities are introduced to the controller as input using linguistic terms. The input values are then converted to fuzzy values using membership functions. This step is called fuzzification. These values perform the classification between input and output. The next step is decision-making, which refers to using predetermined rules to correlate the fuzzy input values to fuzzy outputs. In the last step, the output values are defuzzified; they are converted to values that can be used as control actions.

Fuzzy theory can be applied to determine the desired control force to be applied by the actuator. Neural network performance function selection can be used in structural control Casciati et al. (1993).

4.6 H_2/H_∞ Control Algorithm

The goal of $\mathbf{H_2/H_\infty}$ control algorithms is to design a controller that minimizes the H_2 or H_∞ norm of the closed-loop transfer function matrix, H, from the disturbance to the output vector.

The H_2 norm of a stable transfer function matrix is,

$$\left\|\mathbf{H}\right\|_2 = \sqrt{trace\left\{\frac{1}{2\pi}\int_{-\infty}^{\infty}\mathbf{H}(j\omega)\mathbf{H}^*(j\omega)d\omega\right\}} \tag{27}$$

More details regarding the use of control H_2 and LQR methods for civil engineering applications can be found in Zacharenakis et al. (2001).

5 Active control systems

5.1 Active tendon system

The active tendon system comprises prestressed cables or diagonal bracings that can be activated axially by servo-controlled hydraulic or electromagnetic actuators Reinhorn et al. (1989). It is ideal for steel structures since it is based on diagonal structural elements that already exist and are used passively in this type of structure. This active control device can work against many dynamic loads, such as earthquakes and wind.

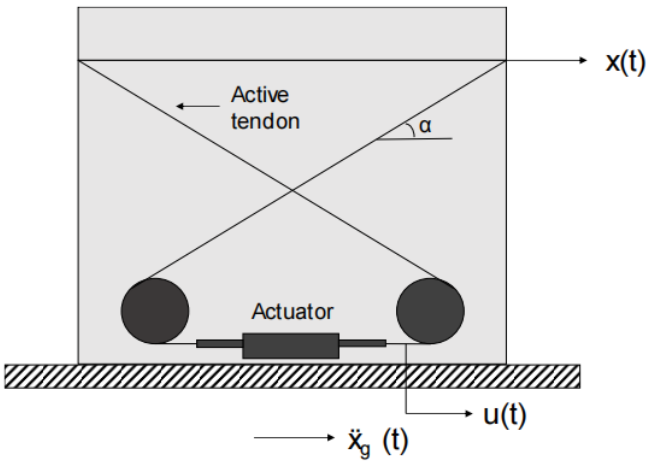

Figure 22. Overview of an active tendon system (Reinhorn AM 1989)

The layout of the active tendon system is relatively simple. It consists of pretension diagonal tendon cables attached to the frame structure, continuously tensioned by a servo-controlled hydraulic actuator receiving its commands from a microcomputer. In this case, the control force is applied to the structure through the tendons even though there is an actuator. One of the significant advantages of this system is the capability to control multiple levels with only one actuator, as shown below. This is achieved using a system of pulleys, distributing the movement perpetually on each floor.

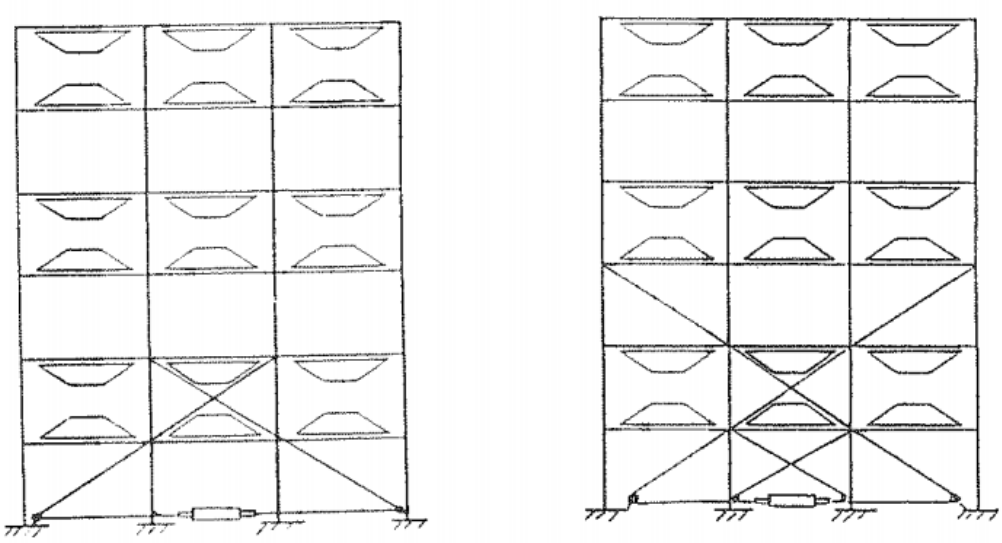

Figure 23. Left : single force control in strong direction Right : proportional control in strong direction (Reinhorn AM 1989)

5.2 Active bracing system

These systems are placed in existing structural braces to create an active control system by adding an actuator. There are three types of active bracing systems (diagonal, K-braces and X-braces). Hydraulic actuators capable of generating much control force are mounted in these braces.

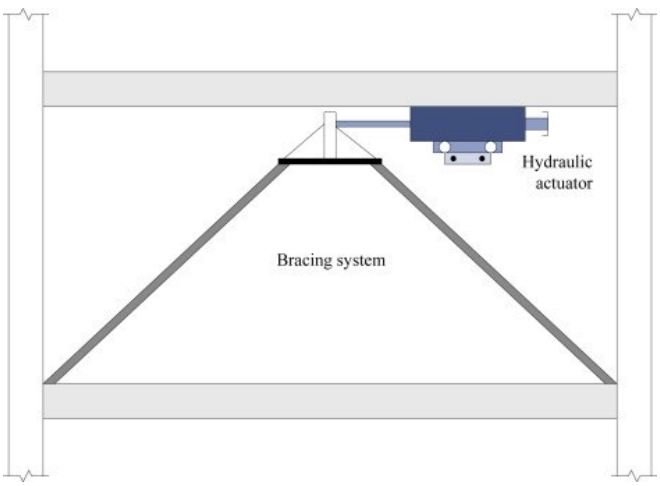

Figure 24. Diagonal active bracing system Franklin et al. (2008).

The actuator applies the control force to the bracing system, which applies it to the structure by longitudinal expansion and contraction during a seismic event or other dynamic load applied to the building Ayşegül et al. (2023). The materials used for construction are steel, concrete and wood. In structures more than 60 storeys high, the construction material is mainly steel Ali (2019).

5.3 Active mass damper

The active mass damper is an extension of a tuned mass damper with the addition of an active control mechanism Naveed et al. (2016). It uses a mass-spring-damper system combined with an actuator that moves the mass as needed to increase the amount of damping and the operational frequency range of the device Pnevmatikos and Gantes (2014).

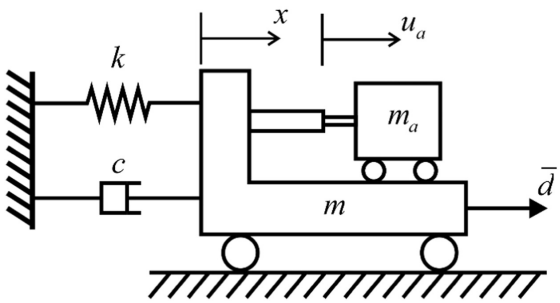

Figure 25. Overview of an active mass damper system (Franklin Y. Cheng 2008)

The main categories of active mass dampers are mechanical, viscous-electric and electric. In its mechanical form, the AMD can only be installed with the ability for post-application in structures. It could perform better for eigenperiods 0.2-1 second because it requires an incredible amount of space due to its large size. It can apply a large amount of force and does not require a liquid tank.

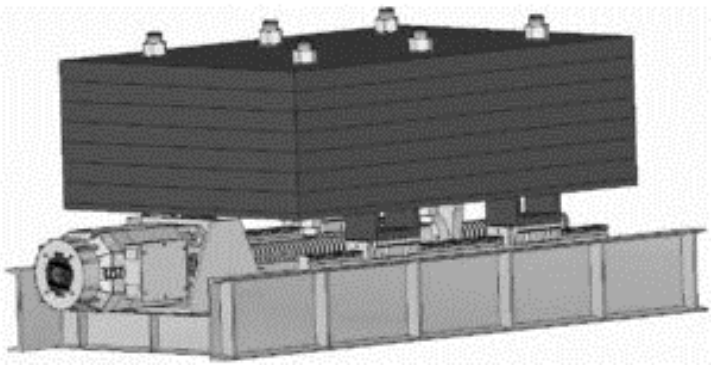

Figure 26. Mechanical AMD (https://deicon.com/ n.d.)

Viscous-electric AMDs are the cutting edge of this type of technology. The use of magnetorheological fluids to alter the dynamic characteristics of the damper based on the excitation. They are significantly easy to install pre and post-construction of a building with a good performance for structures with an eigenperiod of 0.2-1 second. This means they are applicable in most cases of 2- to 10-storey buildings, making them ideal for multi-story housing. They are relatively small regarding the size of the mechanical ones, but they have a small force capacity, and because of the MR fluid, they require the installation of a liquid tank.

Figure 27. I-Pro 1 device by ISAAC Antiseismica (https://isaacantisismica.com/ n.d.)

Electric AMDs use electromagnetic fields to move the actuator into the desirable place each time. They are straightforward to install before and after the construction of the building. Their sibling is viscous-electric, so they perform well in eigenperiods 0.2-1 second. Most are large devices, resulting in ergonomic problems, but many small devices can be used instead. They have a small force capacity and do not require a liquid tank.

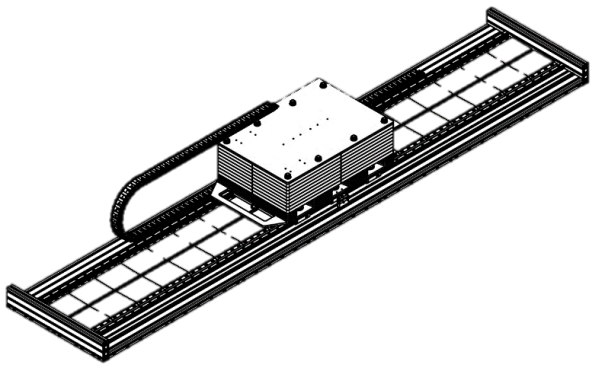

Figure 28. Electro-Pro device by ISAAC Antiseismica (https://isaacantisismica.com/ n.d.)

6 Active mass damper application in steel structures with commercial software

6.1 Active mass damper application software

The Italian company ISAAC, located in Milan, Italy, began as a Polytechnico di Milano spinoff company. It has developed two devices and five analysis software for active mass damper applications, FEA, seismic vulnerability analysis and response spectrum generation (https://isaacantisismica.com/). It has applied its devices successfully domestically and abroad and aims to promote seismic isolation as the modern method of counteracting seismic events.

AMDesign is the active mass damper application software that analyses structures equipped with the company's devices and compares the uncontrolled and controlled structures, enabling engineers to assess whether seismic isolation is needed. In this case, the software was used to apply the ISAAC I-Pro 1 v1.0 with a force capacity of 50KN device in steel structure models. This means that if the control force **F** exceeds this limit, the device cannot apply the force demanded to the structure. As a result, the system's damping is expected to be smaller. The earthquake signal was the El-Centro, California 1940 accelerogram on a 1:1 scale. The signal has a duration of 53.76s with PGA=0.348g.

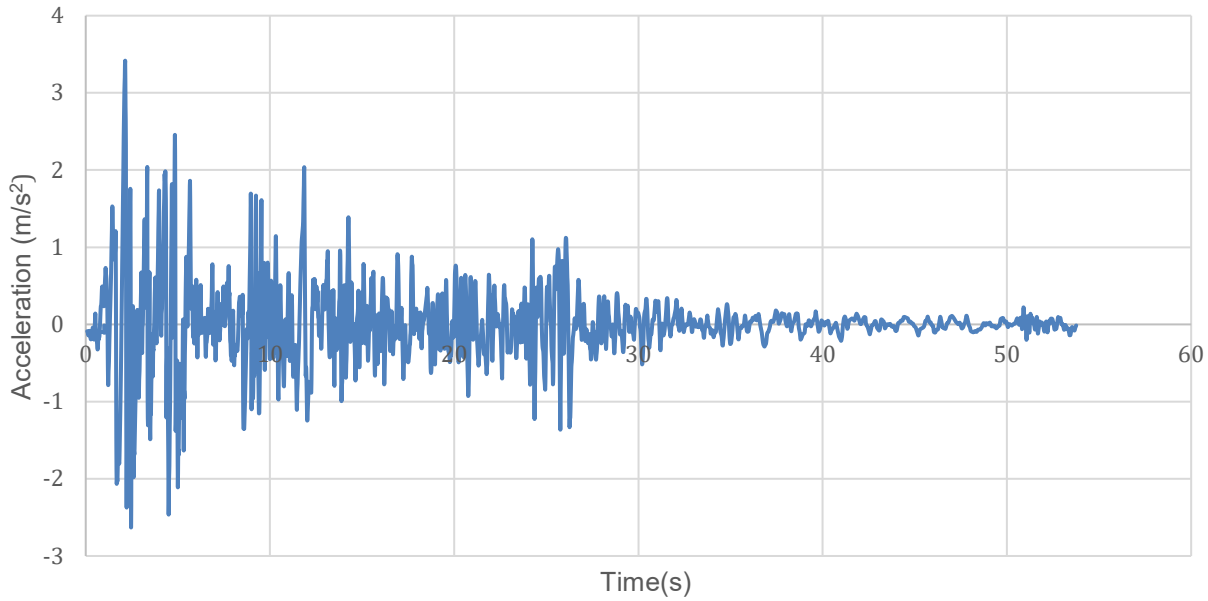

Figure 29. Time history of El Centro, California 1940

6.2 Case study No.1 : Symmetrical steel structure

The first model consists of a five-story symmetrical steel structure with concrete slabs. The optimal solution for the structure was the placement of four devices on the roof. The devices can counteract

the excitation along their longitudinal axis (direction of the arrows). For this reason, two devices were placed perpendicularly to counteract both earthquake components in the X and Y axis. The ideal case is one control device placed on each floor. However, this could cause ergonomic problems regarding the daily use of the building. The mass of the uncontrolled building is 232t, and the period of the single degree of freedom system is 0.55sec.

	Sections	Material
Columns	HEB 400	S235
Beams	HEA 300	S235
Slabs	20cm thickness	C30/37
Wind beams	TUBO 180X180X10	S235

Table 1. Materials and sections of the symmetrical structure

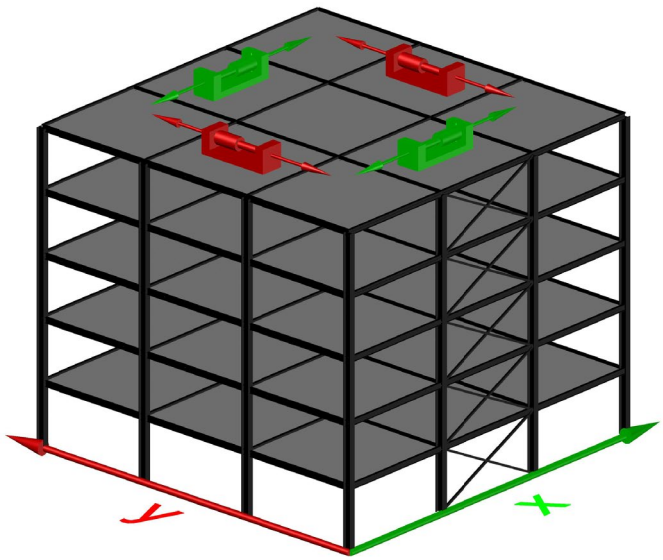

Figure 30. Layout of the symmetrical structure equipped with two devices in each direction

The response of the system showed a significant reduction in all its quantities. The percentage reduction for each axis is displayed below in tabs 2 and 3.

Floor Level	Displacements	Velocities	Accelerations
0	0%	0%	0%
1	22%	28%	1%
2	23%	26%	2%
3	26%	22%	5%
4	28%	17%	9%
5	29%	15%	17%

*Table 2. Percentage reduction of response quantities along **x-axis***

Floor Level	Displacements	Velocities	Accelerations
0	0%	0%	0%
1	30%	28%	7%
2	31%	43%	10%
3	31%	55%	14%
4	32%	38%	29%
5	33%	32%	29%

*Table 3. Percentage reduction of response quantities along **y-axis***

The response of the system for the x-axis is displayed below in Figures 28-30.

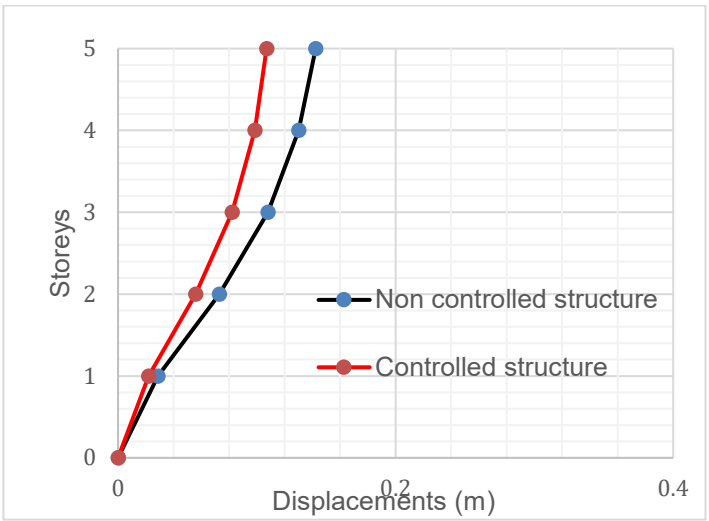

Figure 31. Relative displacements for the symmetrical structure

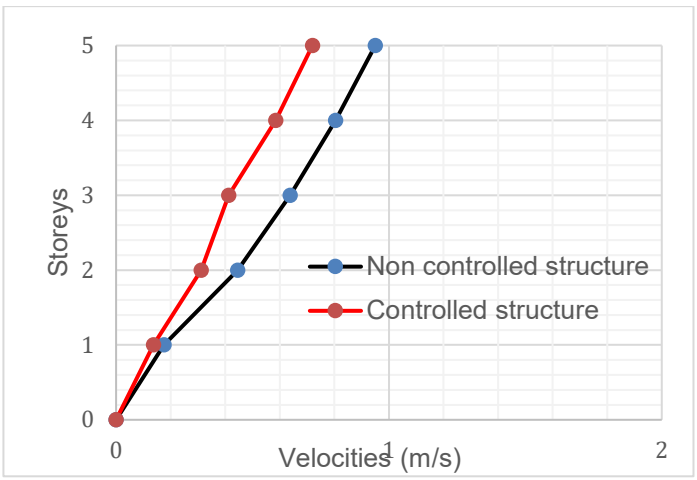

Figure 32. Relative velocities for the symmetrical structure

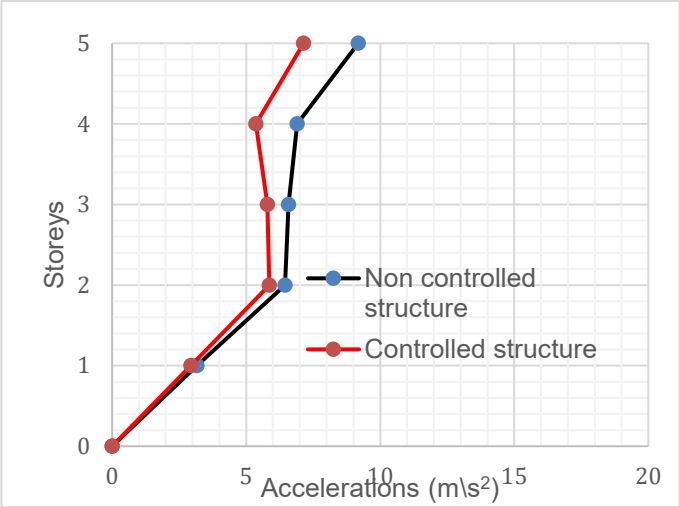

Figure 33. Relative accelerations for the symmetrical structure

The base reaction was reduced to 15% for the y-axis and 7% for the x-axis. The time history plot for the base reaction along each axis is displayed below in Fig.31.

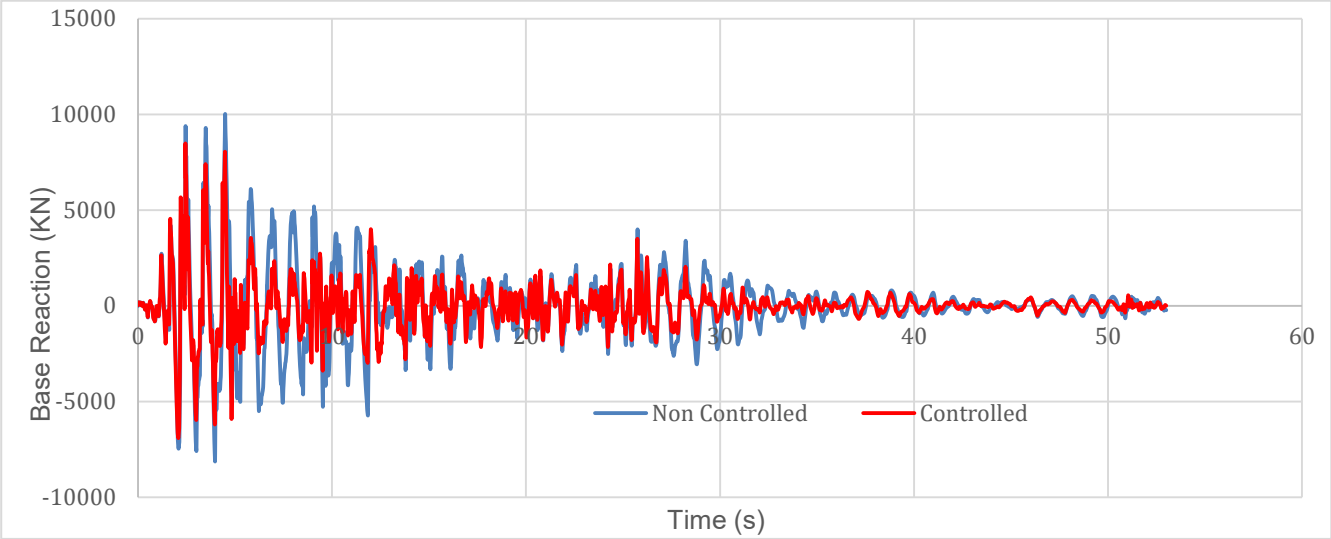

Figure 34. Time history plot for the base reaction along y-axis

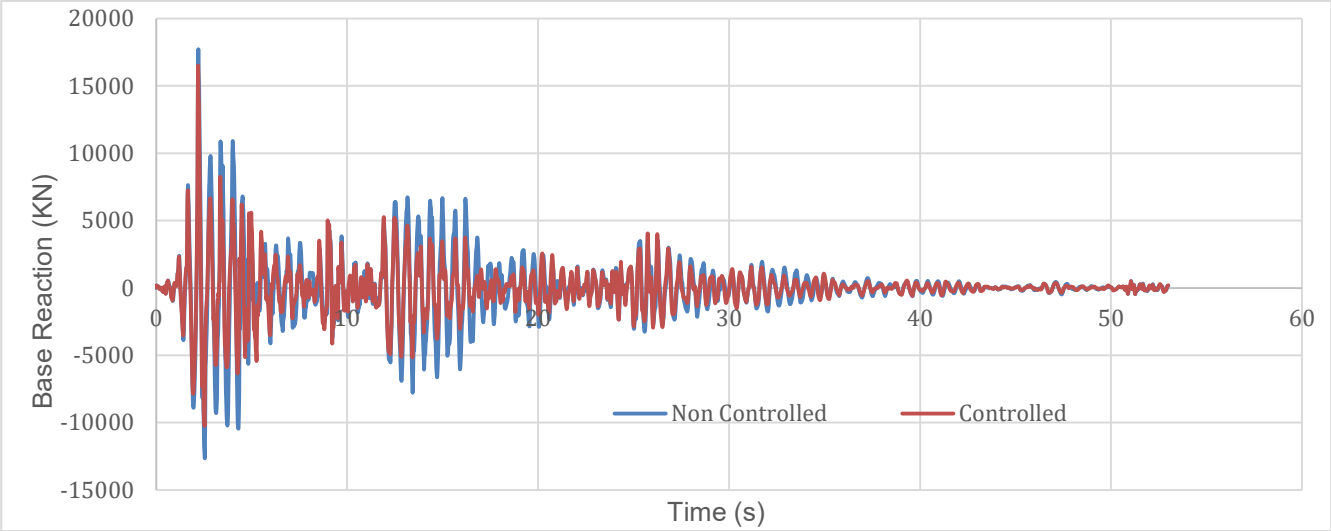

Figure 35. Time history plot for the base reaction along x-axis

6.3 Case study No.2: Non symmetrical steel structure

The second case study also comprises a five-story, non-symmetrical steel structure with concrete slabs. Parametric analyses were conducted regarding the placement and orientation of the AMDs along the floors. The results showed interesting facts about the system's effectiveness in these combinations. The mass of the uncontrolled structure is 129t, and the period of the single degree of freedom system is 0.53sec. The materials and sections used in the structure are the same as above, displayed in Tab.1.

In the first model, two devices were placed on the fifth floor in such a way as to counteract the seismic excitation for each axis. The control nodes in this model were chosen because, in non-symmetrical structures, the frames with minor overall stiffness have larger response quantities than the denser regions due to inertial forces. The layout of the first model is displayed below in Fig. 33.

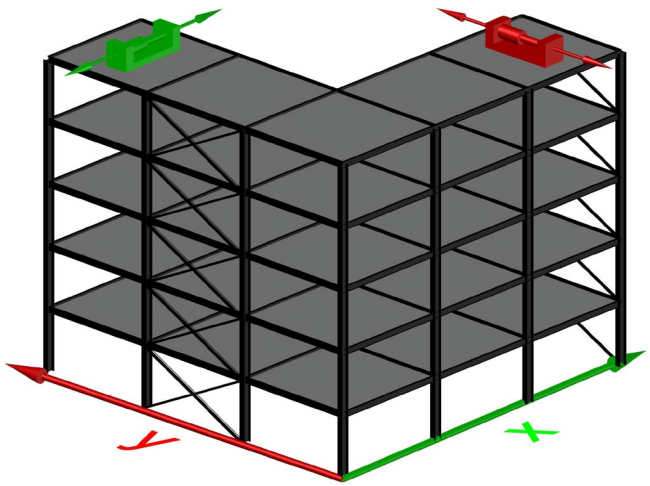

Figure 36. Layout of the first model of Case study No.2

The percentage reduction of the response quantities for each floor is displayed below in Tabs 4-5.

Floor Level	Displacements	Velocities	Accelerations
0	0%	0%	0%
1	18%	36%	4%
2	19%	39%	7%
3	24%	42%	12%
4	29%	28%	27%
5	39%	19%	27%

*Table 4. Percentage reduction of the response quantities for the first model of Case Study No.2 along **y-axis***

Floor Level	Displacements	Velocities	Accelerations
0	0%	0%	0%
1	17%	20%	3%
2	17%	21%	6%
3	17%	21%	15%
4	17%	21%	30%
5	17%	20%	34%

*Table 5. Percentage reduction of the response quantities for the first model of Case Study No.2 along **x-axis***

In the second model, the devices were placed at the same control nodes as in the first, but on the fifth and first floors. The examination of this model shows whether the placement of control devices in the lower floors reduced the response quantities further than in the previous model. The layout of the second model is displayed below in Fig. 34.

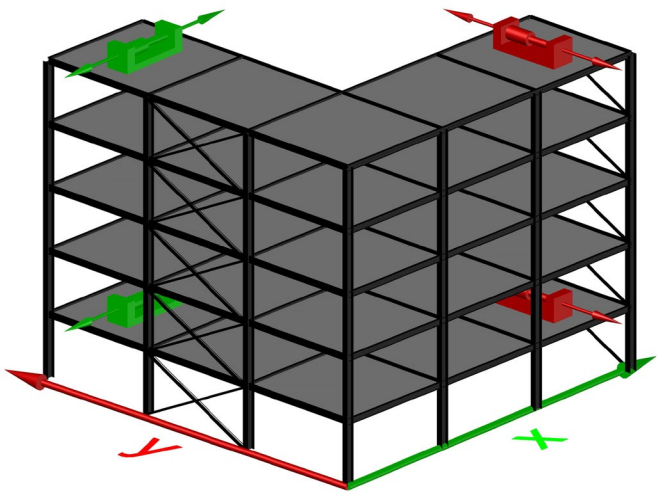

Figure 37. Layout of the second model of Case Study No.2

The percentage reduction of the response quantities for each floor is displayed below in Tabs 6-7.

Floor Level	Displacements	Velocities	Accelerations
0	0%	0%	0%
1	16%	17%	2%
2	17%	17%	5%
3	18%	13%	9%
4	18%	13%	12%
5	18%	12%	15%

*Table 6. Percentage reduction of the response quantities for the second model of Case Study No.2 along **y-axis***

Floor Level	Displacements	Velocities	Accelerations
0	0%	0%	0%
1	34%	36%	9%
2	35%	38%	12%
3	37%	38%	17%
4	40%	33%	18%
5	41%	30%	37%

*Table 7. Percentage reduction of the response quantities for the second model of Case Study No.2 along **x-axis***

The response quantities of the second model are indeed smaller than the first model. This shows that the philosophy explained earlier is valid. Proceeding to the third model was chosen to place the devices in the same orientation but on the fifth and third floors. The layout of the third model is displayed below in Fig. 35.

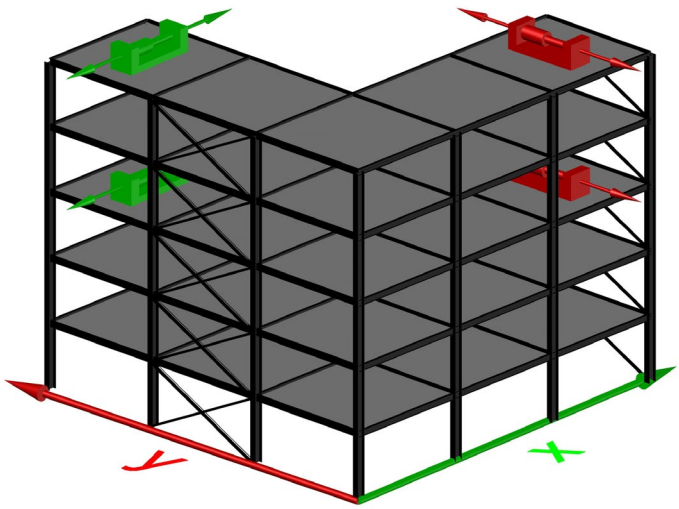

Figure 38. Layout of the third model of Case Study No.2

The percentage reduction of the response quantities for each floor is displayed below in Tabs 8-9.

Floor Level	Displacements	Velocities	Accelerations
0	0%	0%	0%
1	22%	24%	6%
2	24%	26%	9%
3	25%	20%	13%
4	27%	19%	17%
5	28%	18%	20%

*Table 8. Percentage reduction of the response quantities for the third model of Case Study No.2 along **y-axis***

Floor Level	Displacements	Velocities	Accelerations
0	0%	0%	0%
1	40%	45%	12%
2	39%	46%	15%
3	43%	45%	20%
4	45%	40%	23%
5	45%	32%	43%

*Table 9. Percentage reduction of the response quantities for the third model of Case Study No.2 along **x-axis***

For the fourth model, the placement of the devices was appointed to the second and fourth floors. This way, the control of the middle floors is examined to see if the structure responds better than the previous models. The layout of the fourth model is displayed below in Fig. 36.

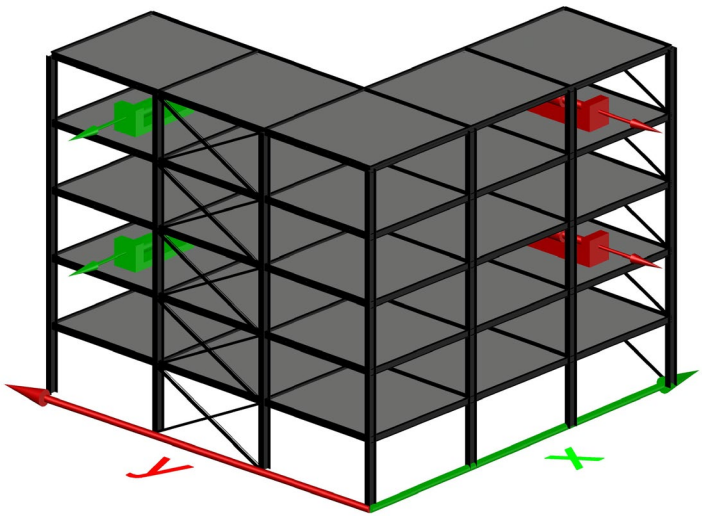

Figure 39. Layout of the fourth model of Case Study No.2

The percentage reduction of the response quantities for each floor is displayed below in Tabs 10-11.

Floor Level	Displacements	Velocities	Accelerations
0	0%	0%	0%
1	17%	15%	5%
2	18%	16%	7%
3	18%	14%	8%
4	18%	13%	11%
5	18%	12%	14%

*Table 10. Percentage reduction of the response quantities for the fourth model of Case Study No.2 along **y-axis***

Floor Level	Displacements	Velocities	Accelerations
0	0%	0%	0%
1	45%	36%	8%
2	43%	38%	10%
3	45%	38%	14%
4	46%	35%	17%
5	45%	31%	40%

*Table 11. Percentage reduction of the response quantities for the fourth model of Case Study No.2 along **x-axis***

The control devices were set along all the floors and orientation for the fifth model. This now means that the seismic signal along the y and x-axis will be counteracted by five machines each. The results are expected to be better than all the previous models. This is a non-realistic application of the devices due to ergonomic problems. However, it can show how the controllability level can significantly change the response of the controlled and uncontrolled structure. The layout of the fifth model is displayed below in Fig. 37.

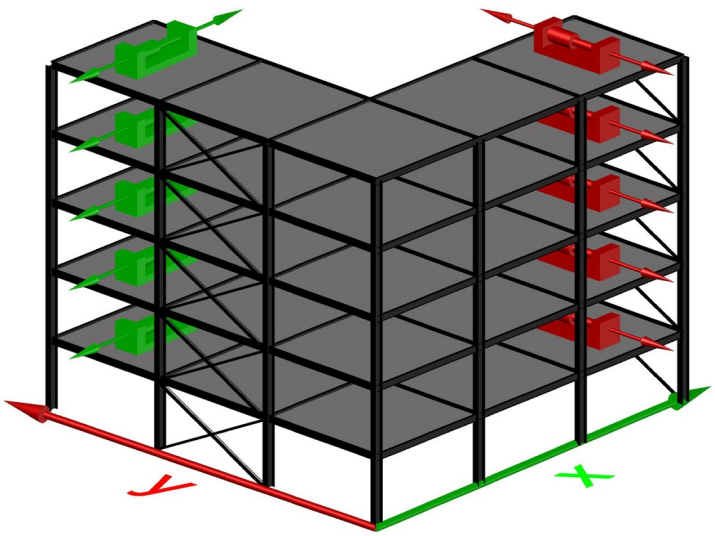

Figure 40. Layout of the fifth model of Case Study No.2

The percentage reduction of the response quantities for each floor is displayed below in Tabs 12-13.

Floor Level	Displacements	Velocities	Accelerations
0	0%	0%	0%
1	22%	24%	6%
2	24%	26%	9%
3	25%	20%	13%
4	27%	19%	17%
5	28%	18%	20%

*Table 12. Percentage reduction of the response quantities for the fifth model of Case Study No.2 along **y-axis***

Floor Level	Displacements	Velocities	Accelerations
0	0%	0%	0%
1	65%	47%	14%
2	63%	51%	19%
3	61%	52%	28%
4	59%	53%	34%
5	58%	50%	60%

*Table 13. Percentage reduction of the response quantities for the fifth model of Case Study No.2 along **x-axis***

As expected, the response of the controlled system is significantly smaller than the previous models. This is why controllability must be a primary issue in applying control devices. This can be seen in the time history of the system's displacements displayed below in Fig 38 and Figs. 39-41.

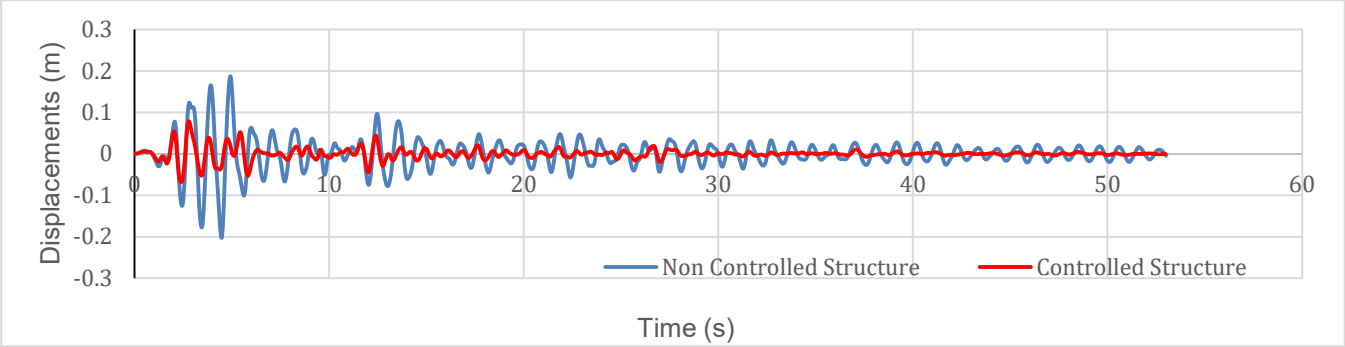

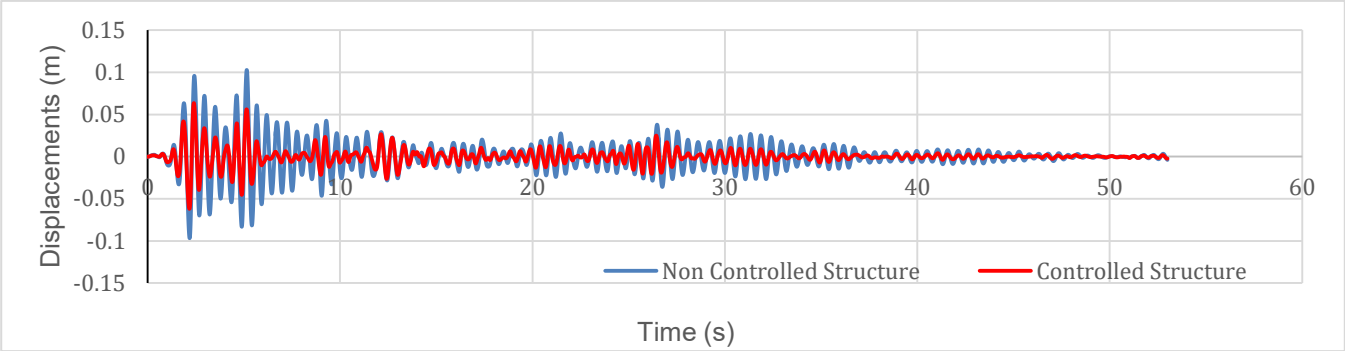

Figure 41. Time history plot for the relative displacements for the sixth model along y and x axis, respectively

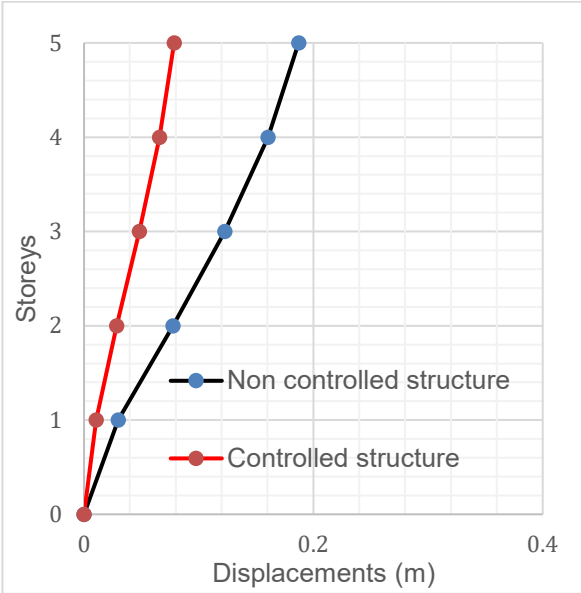

*Figure 42. Relative displacements for the fifth case along each floor for **x-axis***

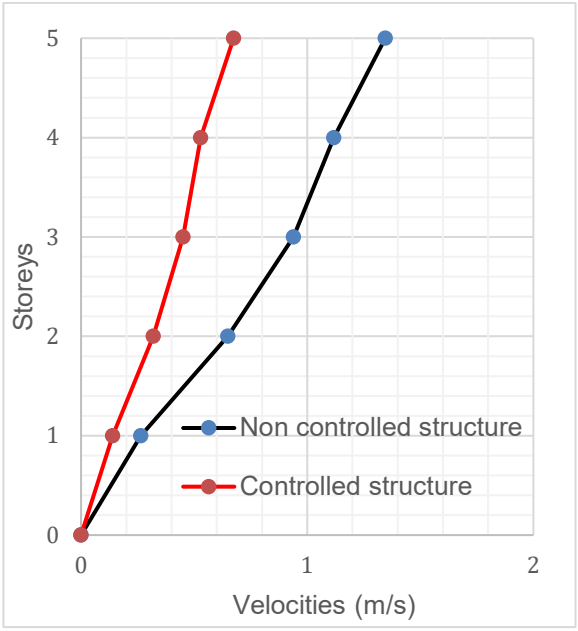

*Figure 43. Relative velocities for the fifth case along each floor for **x-axis***

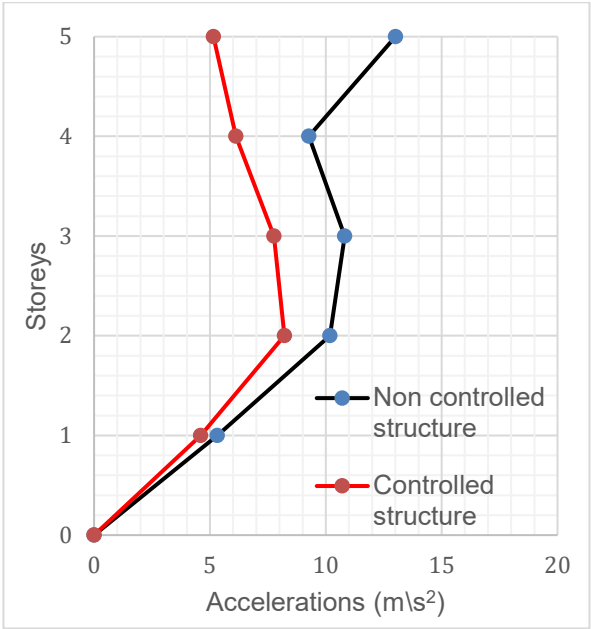

*Figure 44. Relative accelerations for the fifth case along each floor for **x-axis***

For the sixth model, the devices were placed in the two branches' common areas to see the results of controlling the nodes with the maximum stiffness. The layout of the sixth model is displayed below in Fig. 38.

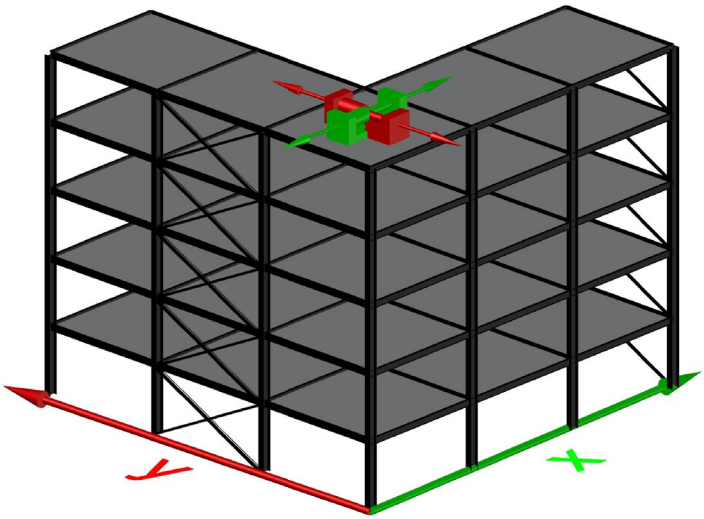

Figure 45. . Layout of the sixth model of Case Study No.2

The percentage reduction of the response quantities for each floor is displayed below in Tabs 14-15.

Floor Level	Displacements	Velocities	Accelerations
0	0%	0%	0%
1	41%	58%	13%
2	45%	54%	12%
3	49%	35%	12%
4	53%	30%	19%
5	55%	27%	27%

*Table 14. Percentage reduction of the response quantities for the sixth model of Case Study No.2 along **y-axis***

Floor Level	Displacements	Velocities	Accelerations
0	0%	0%	0%
1	27%	25%	7%
2	27%	30%	8%
3	30%	34%	11%
4	33%	31%	16%
5	36%	21%	32%

*Table 15. Percentage reduction of the response quantities for the sixth model of Case Study No.2 along **x-axis***

The seventh model keeps the same device-placement philosophy of placing devices where the irregularity happens but adds the third floor to the controlled floors. This achieves the same results as the third model, where the percentage reduction of the response quantities was closer to the fully controlled building of the fifth model.

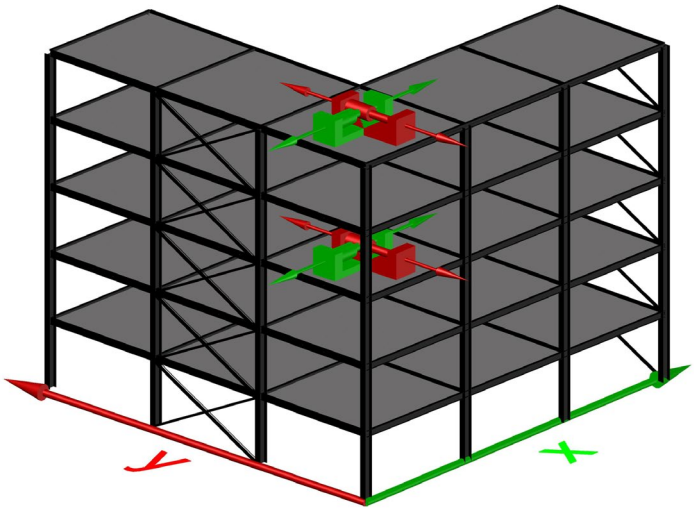

Figure 46. Layout of the seventh model of Case Study No.2

The percentage reduction of the response quantities for each floor is displayed below in Tabs 16-17.

Floor Level	Displacements	Velocities	Accelerations
0	0%	0%	0%
1	36%	28%	-6%
2	40%	31%	1%
3	41%	18%	6%
4	41%	22%	11%
5	41%	19%	15%

*Table 16. Percentage reduction of the response quantities for the seventh model of Case Study No.2 along **y-axis***

Floor Level	Displacements	Velocities	Accelerations
0	0%	0%	0%
1	27%	33%	12%
2	28%	32%	9%
3	30%	30%	9%
4	33%	25%	11%
5	36%	21%	24%

*Table 17. Percentage reduction of the response quantities for the seventh model of Case Study No.2 along **x-axis***

For the eighth model, the controllability level has risen by placing devices in the same configuration as before but along all floors. The difference in the response quantities is expected to be the same as that of the fifth and the third models. However, the fact that the design philosophy is different may produce different results instead.

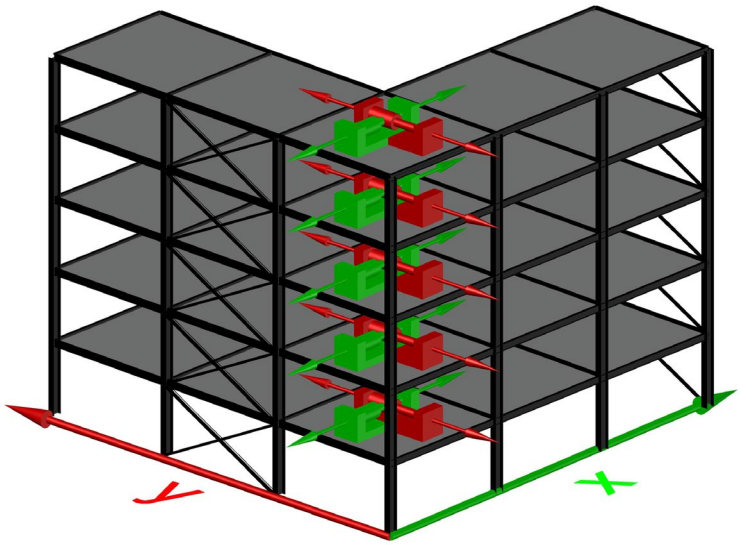

Figure 47. Layout of the eighth model of Case Study No.2

The percentage reduction of the response quantities for each floor is displayed below in Tabs 18-19.

Floor Level	Displacements	Velocities	Accelerations
0	0%	0%	0%
1	48%	48%	5%
2	50%	47%	7%
3	51%	36%	8%
4	52%	37%	15%
5	51%	31%	26%

*Table 18. Percentage reduction of the response quantities for the eighth model of Case Study No.2 along **y-axis***

Floor Level	Displacements	Velocities	Accelerations
0	0%	0%	0%
1	49%	46%	11%
2	51%	50%	16%
3	53%	48%	19%
4	56%	42%	21%
5	58%	37%	34%

*Table 19. Percentage reduction of the response quantities for the eighth model of Case Study No.2 along **x-axis***

As expected, the response quantities are significantly reduced compared to the previous model. In both configurations, meaning the control of the branches versus the common area, the increase of the controllability produces much better results.

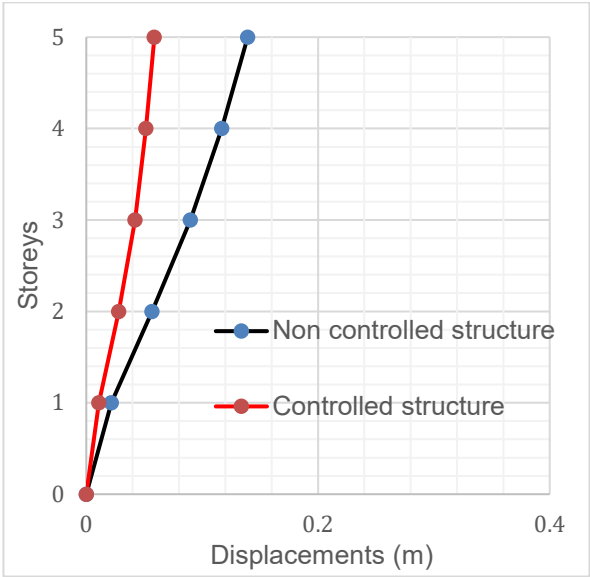

*Figure 48. Relative displacements for the eighth case along each floor for **x-axis***

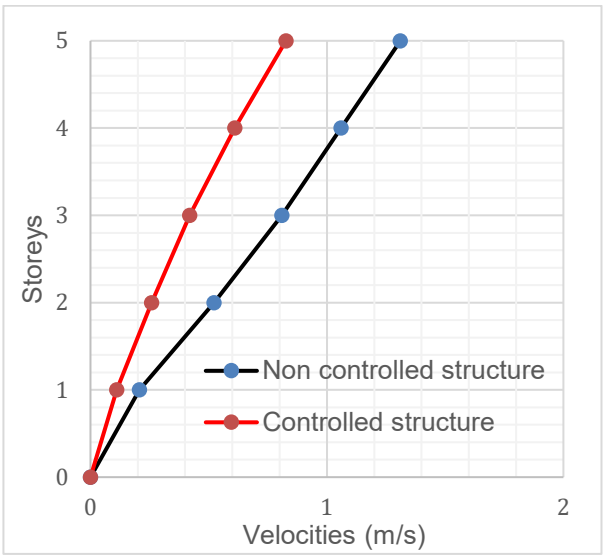

*Figure 49. Relative velocities for the eighth case along each floor for **x-axis***

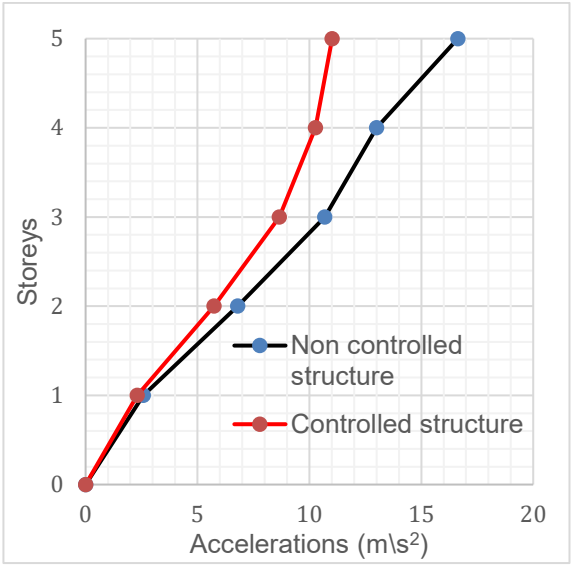

*Figure 50. Relative accelerations for the eighth case along each floor for **x-axis***

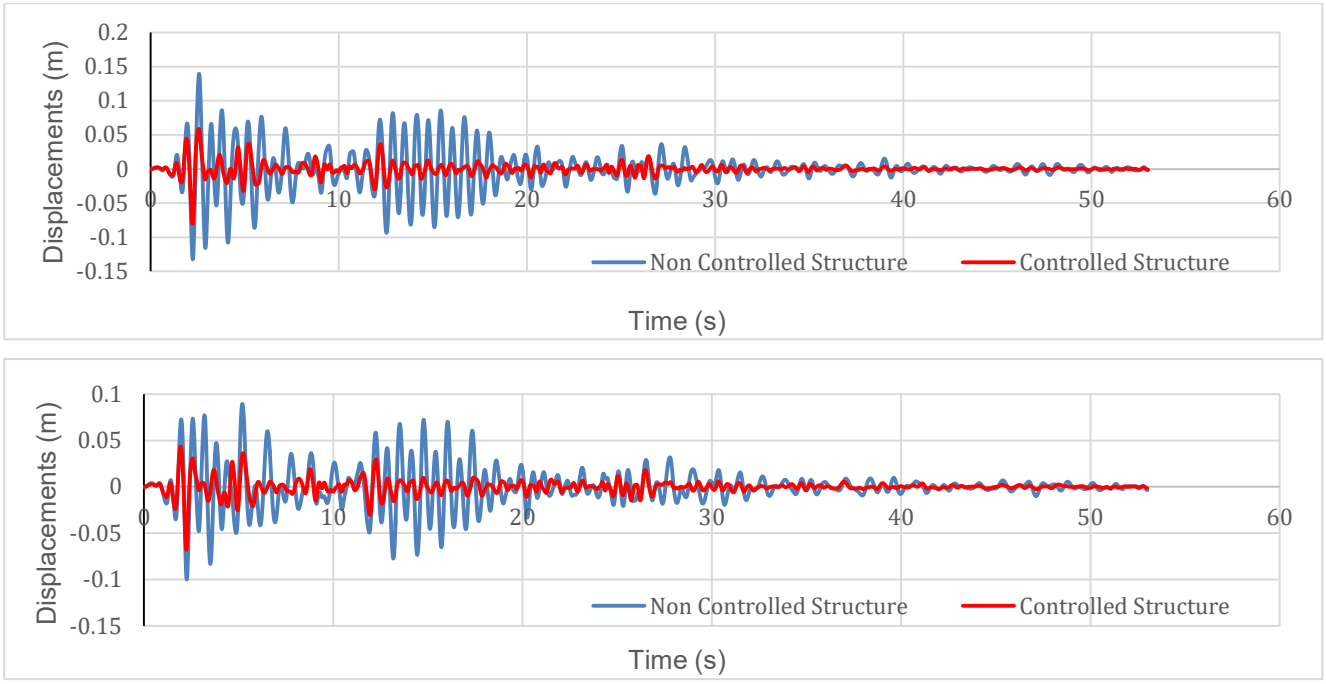

Figure 51. Time history plot for the relative displacements for the eighth model along y and x axis, respectively

In terms of which is the better, the Tabs. 20-21 below shows the difference between the response reductions by subtracting the fifth from the eighth model.

Floor Level	Displacements	Velocities	Accelerations
0	0%	0%	0%
1	26%	24%	-1%
2	26%	21%	-2%
3	26%	16%	-5%
4	25%	18%	-2%
5	23%	13%	6%

Table 20. Difference in percentage reduction of the response quantities by subtracting the fifth from the eighth model for y-axis.

Floor Level	Displacements	Velocities	Accelerations
0	0%	0%	0%
1	-16%	-1%	-3%
2	-12%	-1%	-3%
3	-8%	-4%	-9%
4	-3%	-11%	-13%
5	0%	-13%	-26%

Table 21. Difference in percentage reduction of the response quantities by subtracting the fifth from the eighth model for x-axis

The results show that for the y-axis, the control is more efficient in areas with more considerable stiffness. This happens because of the presence of braces due to the orientation of the steel columns. The controlled response of the system is mainly based on the devices. This equilibrium changes for the case of the x-axis, where the absence of braces and the orientation of the columns, so that they will counteract the seismic excitation by the ductility provided by the strong axis, increases the effectiveness of the control devices that behave better when placed at the area where the stiffness of the building is more minor.

6.4 Base reaction

None of the above would matter without implementing the base reaction reduction. The ultimate goal of applying control devices is to reduce the overall stresses and moments in the primary structural parts. Base reaction refers to the base shear force of the structure obtained by modal response spectrum analysis.

So, the percentage reduction of the base reaction is displayed below in Figs. 49-50.

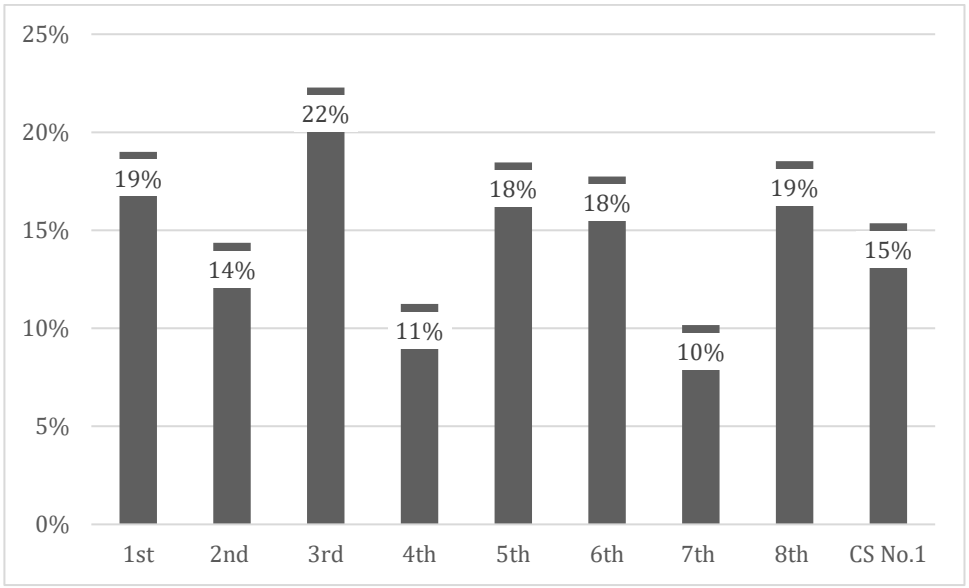

Figure 52. Percentage reduction of the base reaction for x-axis of Case Study No 2.

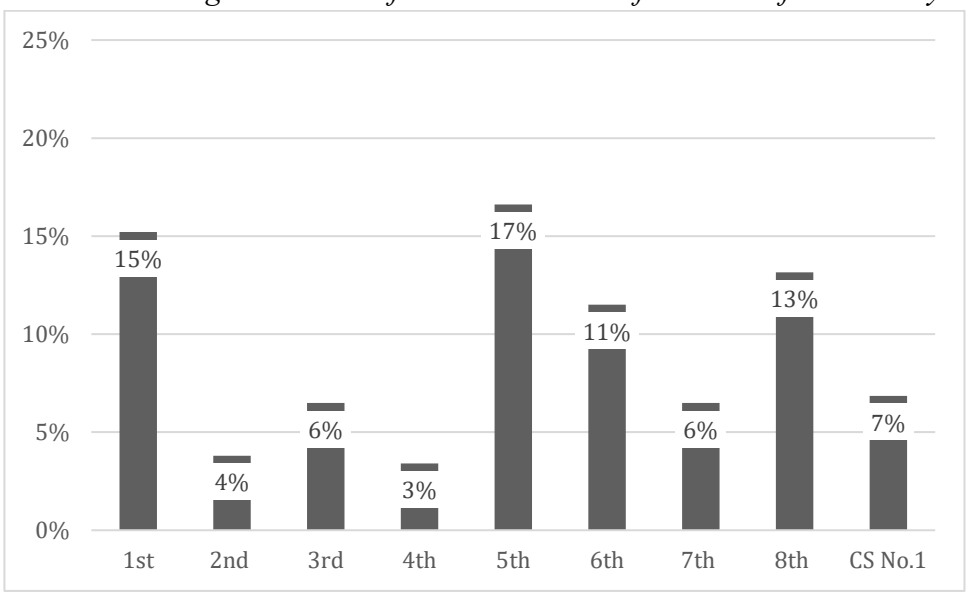

Figure 53. Percentage reduction of the base reaction for y-axis of Case Study No 2.

While the time history plots for the fifth model along x and y axis are displayed below in Figs. 50-51.

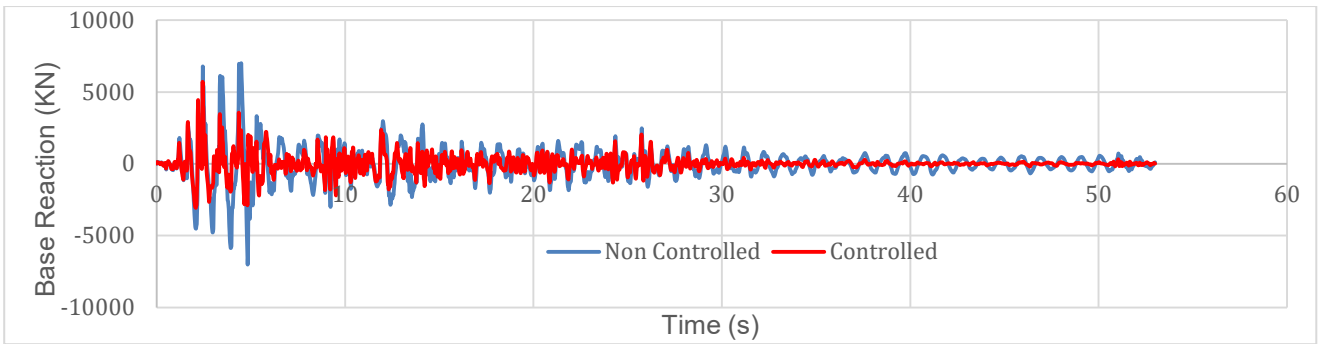

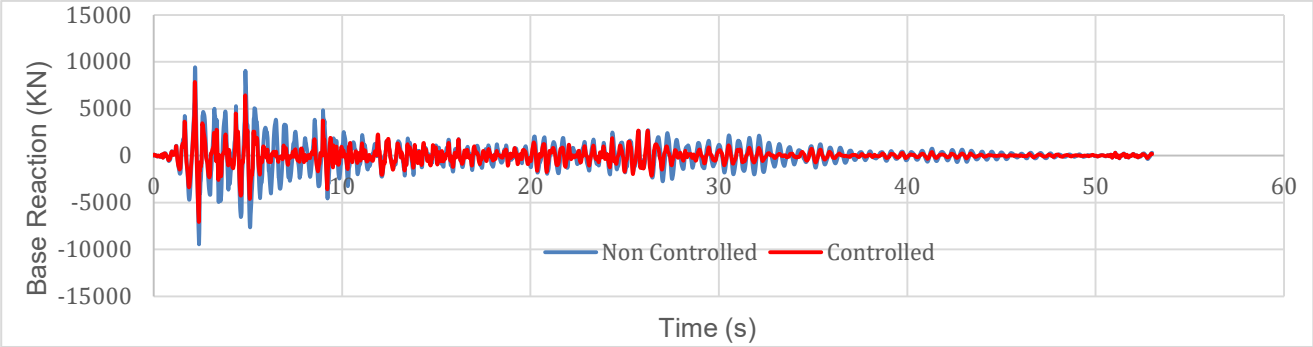

Figure 54. Time history plot for the base reaction along y and x axis, respectively, for the fifth model.

It is exciting that even though the more significant percentage reduction of the response quantities belongs to the fifth model with the increased level of controllability, the base reaction is mainly reduced in the third model. This happens because of the control of the nodes that exhibit a higher rate of response quantities. It is also clear that, around the ''strong'' axis of the structure, the base reaction is significantly reduced compared to the direction where braces are placed.

6.5 Control force saturation

As mentioned in Chapter 3.3, the active mass dampers have a limit in the force that they can apply to the structure. This is called saturation capacity. The device applied to the structures had an allowable force of 50KN, so the algorithm was implemented with the modification of Eq.12, as displayed below.

$$sat\mathbf{F}_{(t-\,td)} = \begin{cases} \mathbf{F}_{(t-\,t_d)} & \left|\mathbf{F}_{(t-\,t_d)}\right| < 50 \\ \mathbf{F}_{\text{allowable}} & \left|\mathbf{F}_{(t-\,t)}\right| > 50 \end{cases} \tag{28}$$

During the seismic event, the force may exceed the device's limits. This does not mean the device will not perform and reduce the response quantities as expected. All the results displayed above are products of this limitation. Figs. 51-52 have a better overview of the control force saturation during

the 53s earthquake signal.

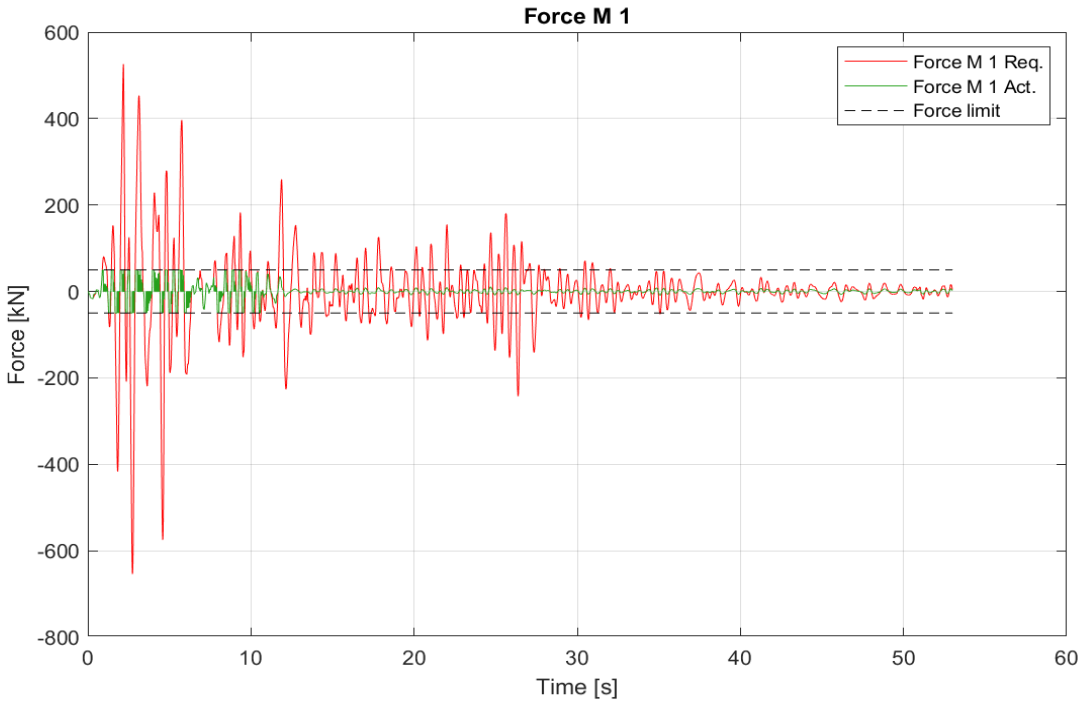

Figure 55. Force saturation of the device placed on the fifth floor of fifth model along x-axis

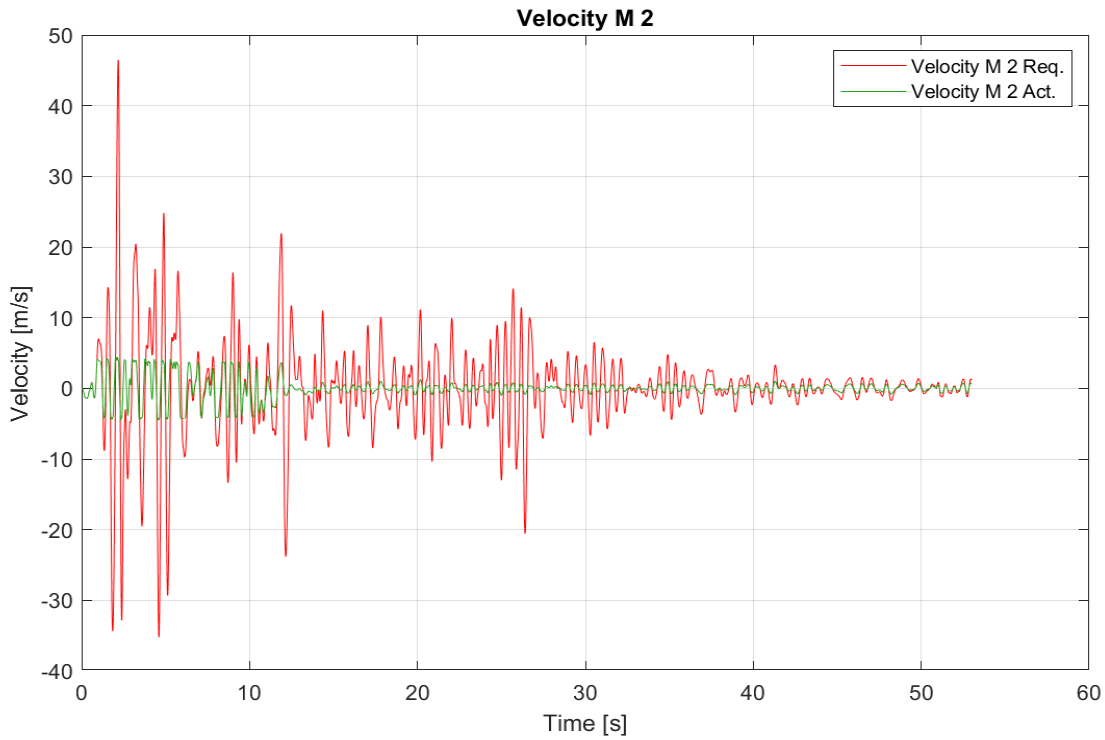

Figure 56. Saturation regarding the velocity of the device placed on the fifth floor of fifth model along y-axis

7 Summary and conclusions

In this thesis, a category of structural active control was introduced by applying different configurations of active mass dampers in two different cases of steel structures. The first case study consisted of one model, while the second consisted of eight models. In the second case, two different application philosophies were implemented. The first application philosophy is the control of the branches of an irregular steel structure, while the second is controlling the maximum stiffness area of the steel structure. The results showed that the first application philosophy performs better in most cases. The second application philosophy only performs better in cases of significant stiffness difference due to reduced ductility in steel section orientation, where braces are placed. The thesis produced the following conclusions:

1. Active control devices can significantly reduce the response quantities of a steel structure.
2. Structural control can be implemented as a base reaction reduction method in earthquake design cases.
3. Steel structures equipped with active control devices behave differently regarding the direction of the excitation due to the irregular shapes of sections.
4. The placement of control devices on the upper floors and combinations of them may perform better than placing them on each floor. This can be a topic for further investigation and research regarding the optimal application of active control devices in steel structures.

8 References

1. https://deicon.com/solutions/tuned-mass-dampers/active-tuned-mass-dampers-active-mass-dampers/.

2. https://isaacantisismica.com/en/active-protection/.

3. Abdel-Rohman M., Quintana V.H., Leipholz H. 1980. "Optimal control of civil engineering structures." *Journal of Engineering Mechanics Division ASCE* 57-73.

4. Ali, Ali Hussein. 2019. "Performance of diagonals in high rise steel structures." *International Journal of Civil Engineering and Technology.*

5. Ayşegül Erdoğan, Süleyman İpek, Esra M. Güneyisi. 2023. "Seismic protection strategies for damage mitigation in structures." 307-342. Woodhead Publishing, ISBN 9780323885300.

6. Carlson JD, Catanzarite DM, St Clair KA. 1995. "Commercial magneto-rheological fluid devices." *Proceedings of the 5th international conference on ER fluids, MR fluids and associated technology.* Sheffield: University of Sheffield.

7. Casciati F, Faravelli L, Venini P. 1993. "A neural-network performance-function selection in active." *Proceedings of the international workshop on structural control.* Los Angeles: University.

8. Casciati F, Magonette G, Marazzi F. 2006. *Technology of semiactive devices and applications in.* Chichester: Wiley ISBN 978-0-470-02289-4.

9. Chu SY, Soong TT, Reinhorn AM. 2005. *Active, hybrid, and semi-active structural control a design.* United Kingdom: Wiley.

10. Constantinou MC, Symans MD, Tsopelas P, Taylor DP. 1993. "Fluid viscous dampers in applications." San Fransisco: ATC-17-1 seminar on seismic isolation.

11. Don-Ho Yang, Ji-Hwan Shin, HyunWook Lee, Seoug-Ki Kim, Moon K. Kwak. 2017. "Active vibration control of structure by Active Mass Damper and Multi-Modal Negative Acceleration Feedback control algorithm." *Journal of Sound and Vibration* 18-30.

12. Dyke SJ, Spencer BF, Sain MK, Carlson JD. 1996. "Modeling and control of magnetorheological." *Smart Mater Struct* 565–75.

13. Ehrgott RC, Masri SF. 1992. "Modelling the oscillatory dynamic behavior of electrorheological." *Smart Mater Struct* (Smart Mater Struct) 275–285.

14. Emmanouil Ioannis Daktylidis, Aikaterini Koursari, Constantinos Repapis, Nikolaos Pnevmatikos. 2023. "Active mass damper application in steel structures." *10th National Conference on Steel Structures*, Athens: Steel Structures Research Society.

15. Emmanouil Ioannis Daktylidis, Constantinos Repapis, Nikolaos Pnevmatikos. 2024. "Control algorithm application in structures subjected to earthquake excitation." *World Conference on Earthwquake Engineering.* MIlan.

16. Erhrogott RC, Marsi SF. 1993. “Structural control applications of an electrorheological device.” *Proceedings of the international workshop on structural control.* Honolulu. 115–129.

17. Feng MQ, Shinozuka M. 1992. *Experimental and analytical study of a hybrid isolation system using.* Buffalo: National center for earthquake engineering.

18. Franklin Y. Cheng, Hongping Jiang and Kangyu Lou. 2008. *Smart Structures – Innovative systems for seismic.* Edited by Taylor & Francis Group. CRC Press.

19. Housner G.W., Marsi S.F., Chassiakos A.G. 1997. *1st World Conference on Structural Control.* California.

20. JJ, Connor. 2003. “Introduction to structural motion control.” *Mit-prentice hall series on civil, environmental, and system.* Prentice Hall, USA.

21. Kautsky, J., and Nichols N.K. 1985. “Robust Pole Assignment in Linear State Feedback.” *International Journal of Control* (41): 1129-1155.

22. Kobori T, Takahashi M, Nasu T, Niwa N, Ogasawara K. 1993. “Seismic response controlled structure.” *Earthquake Eng Struct Dyn* 925–941.

23. Kobori T., Inoue Y., Seto K., Iemura H. Nishitani A. 1998. *2nd World Conference on Structural Control.* New York.

24. Kose I.E., Chmitendorf W.E., Yang J.N. 1995. “H control for seismic-excited building with acceleration feedback.” *Journal of Engineering Mechanics ASCE* 994-1002.

25. LA, Zadeh. 1965. “Fuzzy sets.” In *Info Control*, 8:338–353.

26. Laub, A.J., and M. Wette. 1984. “Algorithms and Software for Pole Assignment and Observers.” In *UCRL-15646 Rev.1*, edited by EE Dept. California: University of California Santa Barbara.

27. Lin C, Chen L, Chen C. 2007. “Hybrid control for MIMO uncertain non linear system using.” *IEEE Trans Neural Netw* 708–720.

28. Lowinger, Patrick. 2017. 15 February. https://discoveringancienthistory.wordpress.com/2017/02/15/hero-of-alexandria-bringing-the-gods-to-life/.

29. Makris N, Hill D, Burton S, JordanM. 1995. “Electrorheological fluid damper for seismic protection.” *Proceedings of the smart structures and materials.* San Diego. 184–194.

30. Mei, Gang & Kareem, Ahsan & Kantor, Jeffrey. 2002. “Model Predictive Control of Structures under Earthquakes using Acceleration Feedback.” *Journal of Engineering Mechanics ASCE.*

31. Naveed Anwar, Thaung Htut Aung , Fawad Ahmed Najam. 2016. “Smart Systems for Structural Response Control - An Overview.” *5th ASEP Convention on Concrete Engineering Practice and Technology.* Manila, Philippines.

32. Nikos G. Pnevmatikos, George A. Papagiannopoulos, George Hatzigeorgiou. 2016. “Control of structures subjected to earthquake excitation based on non resonance theory.” Sheffield: 6th European Conference of Structural Control.

33. Nikos Pnevmatikos, Charis Gantes. 2014. “Actively and Semi-actively Controlled Structures Under Seismic Actions - Modeling and Analysis.” *Springer Encyclopedia of Earthquake Engineering.*

34. Ogata, K. 1997. *Modern Control Engineering.* 3rd. Prentice Hall International Inc.

35. Ohrui S, Kobori T, Sakamoto M, Koshika N, Nishimura I, Sasaki K, Kondo A, Fukushima I. 1994. “Development of active-passive composite tuned mass damper and an application to the high rise.” *Proceedings of the first world conference on structural control.* Pasadena, California. 100-109.

36. Paul, Anand. 2016. *https://civildigital.com/.* 1 April . https://civildigital.com/base-isolation-system-outline-on-principles-types-advantages-applications/.

37. Pnevmatikos N, Gantes C. 2011. “Influence of time delay and saturation capacity to the response of.” *Smart Struct Syst Int J* 449–470.

38. Pnevmatikos, Nikos G. 2007. Σχεδιασμός μεταλλικών κατασκευών με μεθόδους αυτομάτου ελέγχου. PhD Thesis, Athens: National Technical University of Athens.

39. Reinhorn AM, Soong TT, Lin RC, Wang YP, Fukao Y, Abe H, Nakai M. 1989. *1:4 scale model studies of active tendon systems and active mass dampers for aseismic protection.* NCEER-89-0026.

40. Reinhorn, Andrei & Lavan, Oren & Cimellaro, G. 2009. “Design of Controlled Elastic and Inelastic Structures.” *Earthquake Engineering and Engineering Vibration* 469-479.

41. Soong T.T., Spencer B.F. 2002. “Supplemental energy dissipation: state-of-the-art and state-of-the-practice.” *Science Direct* 24 (3): 243-259.

42. Soong, T.T. 1990. *Active structural control: Theory and practice.* London/New York: Longman Scientific&Technical Wiley.

43. Spencer B.F., Dyke S.J., Sain M.K., Carlson J.D. 1997. “Phenomenological model for megnetorheological dampers.” *Journal of engineering mechanics* 230-238.

44. Spencer BF Jr, Nagarajaiah S. 2003. “State of the art of structural control.” *Struct Eng* 845-856.

45. Sriram N, Satish N, Erik J, Henri G. 2003. “Smart base isolated building benchmark problem.” *16th ASCE engineering mechanics conference.* Seattle: University of Washington.

46. Symans MD, Constantinou MC, Taylor DP, Garnujost KD. 1994. “Semi-active fluid viscous dampers for seismic response control.” Los Angeles.

47. Tasarv, Mustafa. 2019. “Solving Equation of Motion using Newmark Methods.” *Response of a Linear SDOF to an Earthquake Ground Motion*, June.

48. WinslowWM. 1947. “Methods and means for translating electrical impulses into mechanical forces.” *US patent 2,417,850.*

49. Yang J.N., Wu J.C., Agrawal A.K., Hsu S.Y. 1995. “Sliding mode control of seismically excited linear structures.” *Journal of Engineering Mechanics ASCE* 1386-1390.

50. Yang, J.N. 1975. “Application of optimal control theory to civil engineering structures.” *Journal of Engineering Mechanics Division ASCE* 819-838.

51. Yi F, Dyke SJ, Caicedo JM, Carlson JD. 2001. “Experimental verification of multi-input seismic.” *J Eng Mech ASCE* 1152–1164.

52. Zacharenakis E.C., Arvanitis K.G., Soldatos A.G., Stavroulakis G.E. 2001. “LQR, and H2 optimal structural control in antiseismic design.” Thessaloniki: National Mechanics Congress.